Title

Cortical Contributions to Smooth Pursuit Learning

Author

Li, Jennifer Xinge

Publication Date

2011

Cortical Contributions to Smooth Pursuit Learning

by

Jennifer Xinge Li

DISSERTATION

Submitted in partial satisfaction of the requirements for the degree of

DOCTOR OF PHILOSOPHY

in

NEUROSCIENCE

in the

GRADUATE DIVISION

of the

UNIVERSITY OF CALIFORNIA, SAN FRANCISCO

[redacted]

Acknowledgements

First, I want to thank Javier Medina for kindly allowing me to use his cerebellar learning data, first published in Nature Neuroscience 11(10), 2008, in Chapter 2 of this thesis. In addition, the text of Chapter 1 is a reprint of the material as it appears in Neuron 69(1), 2011. The coauthor listed in this publication directed and supervised the research that forms the basis for the dissertation/thesis.

As I look back on my graduate career, I am amazed at how fortunate I have been. My biggest stroke of luck was to choose Steve Lisberger as my graduate advisor. Throughout my graduate career, he has tirelessly motivated, inspired, and challenged me with his creativity and clarity of thought. I hope that my current and future work will reflect his scientific spirit, and ensure that his efforts have not been in vain.

Further, I am grateful to my UCSF thesis committee members, Michael Brainard, Allison Doupe, and Loren Frank, who so often helped me tackle questions from a new perspective, and emphasized “the forest before the trees”, both in science and in life. Special thanks goes to Loren, who was always available to help me structure my thoughts, and was a fount of knowledge for all things computational. Finally, I want to thank Jennifer Raymond for so graciously agreeing to serve as my outside committee member.

This thesis could not have been accomplished without our dedicated veterinary and technical support staff, including Karen Macleod, Elizabeth Montgomery, Darryl Floyd, and Scott Ruffner. Our lab manager, Stefanie Tokiyama, was always a source of reason and order in times of chaos. Dirk Kleinhesslink and David Wolfgang-Kimball repeatedly saved my computer, my data, and my sanity.

Last but not least, I want to thank the members of the Keck Center, in particular the past and present residents of HSE-808, for providing a stimulating and collaborative scientific environment. David Schoppik and Helen Mclendon have been particularly generous with their time and support. I also want to acknowledge some close friends outside of the lab: Vinod Rao, Verena Firpo, Stefanie Lim, and Lily Phuong, who have become like family during my graduate years.

I dedicate this thesis to my parents.

Abstract

For a learned movement to be effective, it must be produced at the appropriate time, but how this is achieved in the brain remains unknown. Smooth pursuit is a simple oculomotor behavior that exhibits temporally specific learning. Upon repeated exposure to a precisely-timed instructive change in target direction, the pursuit system learns to produce an eye movement that peaks around time when the instructive stimulus is expected to appear. The smooth eye movement region of the frontal eye fields (FEF_{SEM}), a motor cortex for smooth pursuit, contains a spatial map of elapsed time since the initiation of pursuit, and is therefore a good candidate for mediating the temporal specificity of pursuit learning. In chapter 1, I describe a series of electrophysiology experiments demonstrating that the FEF_{SEM}, by virtue of its innate representation of time, may serve to incorporate the salient temporal features of the instructive stimulus into the learned eye movement.

Because movements improve and become ingrained with practice, motor learning is inherently a dynamic process. In chapter 2, I explored the neural changes associated with the dynamics of motor learning by comparing how activity in the FEF_{SEM} and a downstream cerebellar locus for pursuit, the floccular complex, emerged and evolved as the animal learned to produce the desired eye movement. My findings suggest that pursuit learning arises from a combination of neural processes with different dynamics of adaptation, and that the FEF_{SEM} and the floccular complex utilize these processes in different ways to support at least partially separate aspects of pursuit learning.

Table of Contents

List of Tables

List of Figures

General Introduction

A vital role of all but the simplest motor circuits is to anticipate, and ultimately adapt to, patterns in the environment. At the heart of motor learning are the questions of "when?" and "for how long?". "When" refers to a measurement of time in the context of a single movement (within-movement). The importance of "when" is apparent to a sleep-deprived teenager, or an incorrigible academic, who must hit the snooze button right before the alarm clock screeches its jarring wake up call. "For how long" reflects the inherently dynamic nature of motor learning evident across repetitions of the desired movement (across-movement). For example, someone playing tennis for the first time may serve the ball too low or too hard. However, after weeks of practice, placing the proper touch on the ball becomes second nature. Our daily actions serve as constant reminder that the ability of neural circuits to operate across multiple time scales allows motor learning to be specific yet versatile.

Numerous brain areas have been implicated in estimating time in the context of a single movement and thus provide some possible neural answers for "when?" (Leon and Shadlen, 2003; Lewis and Miall, 2003; Sakurai et al. 2004), yet none of these neural representations of time have been directly linked to motor learning. Similarly, we have a limited understanding of how the process of motor learning unfolds from changes throughout the neural circuit, both due to the dearth of behavioral paradigms that drive sufficiently rapid motor learning so as to permit reliable recordings from the same neurons continuously throughout the learning process, as well as the scarcity of learning data from multiple brain areas within the motor circuit.

Smooth pursuit, an ocular tracking behavior that serves to stabilize a small moving target on the fovea by matching eye velocity to target velocity, is an excellent model for studying how the within-movement and across-movement dynamics of motor learning arise from the changes within the neural circuit. Much is known about the response properties of neurons at different levels of the pursuit circuit, starting from the representation of visual information in the middle temporal area (MT) (Newsome et al., 1988) and the medial superior temporal area (MST) (Chukoskie and Movshon, 2009), to the formation of the motor command in the pursuit region of the frontal eye fields (FEF_{SEM}) (Tanaka and Lisberger, 2001, 2002) and the cerebellum (Krauzlis and Lisberger, 1994, 1996). Further, the anatomical connectivity of the pursuit circuit has been extensively characterized, thus providing additional insight into the interactions between these different structures (for reviews, see Krauzlis, 2004; Sharpe, 2008). Finally, robust smooth pursuit learning can be easily and rapidly induced using a basic experimental setup. Rhesus macaques repeatedly presented with an instructive change in target direction occurring at a fixed delay after target motion onset will rapidly learn to produce a eye movement that is in the direction of the expected change in target trajectory (Medina et al., 2005). A salient feature of the learned eye movement is that it is maximal around the expected onset of the instructive stimulus, thus providing an opportunity for asking how within-movement temporal precision is achieved in the brain. Moreover, the learned eye velocity usually ceased to change after 20 to 40 movement repetitions, which generally corresponded to a few minutes of absolute time in the experiment. Therefore, it is technically feasible to precisely measure the evolution of neural activity throughout the acquisition of the learned behavior and beyond, to ask how the learning process is supported by changes within the neural circuit.

A number of areas throughout the pursuit circuit could potentially serve as sites of motor learning. One such area is the smooth eye movement region of the frontal eye fields (FEF_{SEM}), a motor cortex for smooth pursuit, located in the fundus of the arcuate sulcus. The FEF_{SEM} is believed to play a major role in regulating the gain of visual-motor transmission (Macavoy et al., 1991; Tanaka and Lisberger, 2001, 2002), which describes the selective gating and enhancement of sensory inputs for driving the motor output. Since learning could arise via a shift in the visual-motor gain, an earlier attempt was made to identify changes in the mean firing rate of FEF_{SEM} neurons when animals participated in a speed-learning paradigm. The study failed to find consistent expression of learning across the FEF_{SEM} population (Chou and Lisberger, 2004), although the authors reported a considerable amount of heterogeneity in the magnitude of learning across individual neurons. One possible explanation for the heterogeneity in neural learning, which was not explored in the 2004 study, is that pursuit learning selectively recruits FEF_{SEM} neurons based on the amount of overlap between the neuron's response properties and the features of the instructive stimulus.

The FEF_{SEM} is unique in the pursuit circuit in that it contains a representation of elapsed time from movement onset; different FEF_{SEM} neurons fire most vigorously at distinct times during each movement, and the population activity is such that all times during the movement elicit maximal responses from a subset of neurons (Schoppik et al., 2008). Therefore, the FEF_{SEM} is a possible source for the within-movement temporal specificity of the learned eye movement produced by the direction-learning paradigm. In Chapter 1, I performed series of single-unit recording experiments in awake behaving rhesus macaques to test the hypothesis that the amount of neural learning evoked by a temporally precise instructive stimulus is related to the innate preference of that FEF_{SEM} neuron for the moment during the pursuit movement corresponding to the onset of the instructive stimulus. In the first experiment, I fixed the time at which the instructive stimulus appeared during the movement and measured the expression of learning in neurons that preferred different times during pursuit. Subsequently, I controlled for variability across neurons by measuring the expression of learning in the same neuron as a function of the timing of the instructive stimulus. In both experiments, the expression of learning was greater in FEF_{SEM} neurons that preferred the timing of the instructive stimulus. Finally, by manipulating target motion to directly generate a mean eye movement that mimicked the magnitude and time course of the mean learned eye movement, I confirmed that the pattern of activation in the FEF_{SEM} during temporally specific pursuit learning was not merely a result of the change in the eye movement, and instead was unique to the learning context. Taken together, these results suggest that the FEF_{SEM} may help produce a learned eye movement with the desired temporal specificity.

The neural circuit for smooth pursuit is composed of two interacting pathways (Lisberger, 2010), both originating in the cortical visual areas MT and MST, which serve distinct functions. The first pathway, which includes the FEF_{SEM}, controls the visual-motor gain. The second pathway bypasses the FEF_{SEM}, and carries image motion that drives changes in eye velocity. Both pathways are believed to ultimately converge upon a number of targets in the cerebellum, including the oculomotor vermis and the floccular complex, where the command for moving the eyes is assembled. Directional pursuit learning elicits changes in the mean firing rate of Purkinje cells in at least one of these cerebellar targets, the floccular complex (Medina and Lisberger, 2008). In Chapter 2, I tested the hypothesis that the FEF_{SEM} and the floccular complex have different roles during pursuit learning by comparing the how activity in the two brain areas evolved across movements as the animal acquired and practiced the learned movement.

I found that although both the FEF_{SEM} and the flocccular complex populations averages had learning dynamics that closely paralleled that of the behavior, the learning dynamics of individual neurons in the two areas diverged from that of the behavior to varying extents, both in the rate of acquisition of the learned response and in its subsequent maintenance. A comparison of these two dynamical features in the learned responses of individual neurons revealed differences between the FEF_{SEM} and the floccular complex, with the latter bearing a closer resemblance to the behavior, perhaps reflecting its closer proximity to the motor output of the pursuit circuit. Therefore, pursuit learning appears to be mediated by multiple neural mechanisms with diverse adaptation dynamics, and the FEF_{SEM} and the floccular complex may perform at least partially separate functions in pursuit learning by engaging these systems in different ways.

Finally, I examined the millisecond-by-millisecond time courses of the mean learned firing rates of neurons from each of the two areas in relation to that of the mean learned eye velocity, and found that although the responses of FEF_{SEM} neurons peaked at different times throughout the duration of the learned eye movement, both the learned eye velocity and the responses of Purkinje cells in the floccular complex followed the same general time course and tended to peak around the onset of the instructive stimulus. Thus, the analysis of the time course of the mean learned neural responses underscores the earlier assertion that the floccular complex may help regulate the amplitude of the learned eye movement, and also reinforces the notion that the FEF_{SEM} may have a special role in specifying the temporal precision of the learned eye movement.

Chapter 1

Learned timing of motor behavior in the smooth eye movement region of the frontal eye fields

1.1 Abstract

Proper timing is a critical aspect of motor learning. We report a relationship between a representation of time and an expression of learned timing in neurons in the smooth eye movement region of the frontal eye fields (FEF_{SEM}). During pre-learning pursuit of target motion at a constant velocity, each FEF_{SEM} neuron is most active at a distinct time relative to the onset of pursuit tracking. In response to an instructive change in target direction, a neuron expresses the most learning when the instruction occurs near the time of its maximal participation in pre-learning pursuit. Different neurons are most active, and undergo the most learning, at distinct times during pursuit. We suggest that the representation of time in the FEF_{SEM} drives learning that is temporally linked to an instructive change in target motion, and that this may be a general function of motor areas of the cortex.

1.2 Introduction

Young children jumping rope soon learn the importance of timing: jumping too early or too late can be as bad as failing to jump at all. Precise timing is critical to all aspects of motor control, at levels ranging from the coordination of joints and muscles during simple reflexive movements to the acquisition of complex skills such as playing a musical instrument. Indeed, timing is so important for motor control that it can be learned. There now are multiple demonstrations that the motor system can learn not just what to do, but also when to do it (Mauk and Ruiz, 1992; Medina et al., 2005; de Hemptinne et al., 2007; Doyon et al., 2009). In the smooth pursuit system, repeated presentations of a precisely-timed instructive change in the direction of a moving target elicits a learned smooth pursuit eye movement that peaks near the time when the instructive motion is expected to occur (Medina et al., 2005).

The ability to learn timing in motor control requires a representation of time during movements. The most relevant temporal signals for motor control are typically on the order of tens to hundreds of milliseconds (Buonomano and Karmarkar, 2002; Mauk and Buonomano, 2004). In eyelid conditioning and smooth pursuit eye movements, learning is largest for an instructive signal that occurs in the range from 200-400 ms after the onset of a conditioned stimulus that references time (Mauk and Ruiz, 1992; Medina et al., 2005). Possible timing signals have been observed via imaging or electrophysiological studies throughout the brain, for example in the basal ganglia (Rao et al., 2001; Chiba et al., 2008; Jin et al., 2009), the cerebellum (Lewis and Miall, 2003; Smith et al., 2003), the prefrontal cortex (Sakurai et al., 2004; Oshio et al., 2006; Jin and

Graybiel, 2009), the supplementary motor cortex (Shih et al., 2009; Onoe et al., 2001), and the parietal cortex (Leon and Shadlen, 2003). The next step is to establish a link between a representation of time and a neural expression of learning.

A prior paper from our laboratory reported a representation of time in the smooth eye movement region of the frontal eye fields (FEF_{SEM}) (Schoppik et al., 2008). Each neuron in the FEF_{SEM} reaches its maximal firing rate at a particular time during pursuit, and the peak responses of the full population tile the entire duration of pursuit. Thus, the representation of smooth pursuit in the FEF_{SEM} is such that each neuron primarily contributes to a particular moment in the eye movement. In contrast, most of the brain regions in the pursuit circuit have stereotyped responses as a function of time during pursuit. Neurons in extrastriate visual area MT tend to have transient responses that are driven by, and time-locked to, the visual motion signals caused by the initial target motion (Newsome et al., 1988). Similarly, Purkinje cells in the cerebellar flocculus show transient responses that are well timed to the onset of target motion, followed by sustained responses that are monotonically related to the smooth eye velocity (Stone and Lisberger, 1990; Krauzlis and Lisberger, 1994).

The unique, temporally-selective representation of pursuit in the FEF_{SEM} raises the possibility we tested here, that this cortical area plays a temporally-specific role in the modulation of pursuit through learning. We recorded changes in the responses of FEF_{SEM} neurons during pursuit learning induced by a precisely-timed instructive change in target direction, to ask whether the learned eye movement would be driven selectively by neurons that contribute to pursuit around the time of the instruction. In agreement with this prediction, we found that the magnitude of learning in any given neuron is correlated with how strongly the same neuron would have responded (during pre-learning pursuit) at the time of the instructive change in target trajectory. We suggest that the representation of time within the FEF_{SEM} may be harnessed to guide the temporal specificity of pursuit learning, and that temporally-specific modulation of motor behavior could be a general function of the motor regions of the cerebral cortex.

1.3 Materials and Methods

Two male rhesus monkeys (*Macaca mulatta*) aged 6 and 8 years, tracked smoothly moving targets in exchange for a water reward. Both monkeys had prior experience in experiments on pursuit, but neither had participated in learning studies. Throughout each experiment, head position was fixed, and eye position in the orbit was monitored using a scleral search coil system. The recording chamber and eye coil were attached during surgery with sterile procedure using approaches described before (Ramachandran and Lisberger, 2005) with the monkey under anesthesia with isofluorane. After surgery, monkeys received analgesics for several days and careful monitoring by veterinary staff. All experimental procedures and protocols used were approved by the *Institutional Animal Care and Use Committee* of UCSF, and are in accordance with use and care guidelines established by the *NIH Guide for the Care and Use of Laboratory Animals*.

1.3.1 Data acquisition

Horizontal and vertical eye positions were sampled at 1 kHz and passed through an analog differentiator with a cutoff of 25 Hz to produce the corresponding eye velocity traces. Quartz shielded tungsten electrodes (Thomas Inc) were lowered anew each day into the frontal eye fields. $\mathrm{FEF}_{\mathrm{SEM}}$ neurons were identified by direction-tuned activity during smooth pursuit, and weak or non-existent responses to saccades or changes in eye position. Spike waveforms were retained using a threshold crossing criterion, and were sorted into single units based on waveform shape and the absence of refractory period violations defined as two waveforms occurring within 1 ms. For a typical recording session, the waveforms from recorded neurons were 3 to 10 times the amplitude of the background noise. Sorted waveforms were converted into spike trains with a temporal precision of 1 ms.

1.3.2 Presentation of visual stimuli

All behavioral experiments took place in a dimly lit room. Visual stimuli were displayed on a BARCO monitor (model number: CCID 7651 MkII) that was placed 40 cm from the eye and subtended 61°x42° of the visual field. Targets were white squares measuring 0.5° along each side. Target motions were presented in discrete trials. Each trial started with a stationary fixation target at the center of the screen for an interval that was randomized between 500 and 1000 ms. Targets then underwent standard step-ramp motion in an unpredictable direction for 750 ms, and then stopped for 500 ms in a second fixation period. For step-ramp motion, the step size was chosen to minimize saccades during pursuit onset and typically ranged between 2° to 3°, depending on the initial direction of target motion. To successfully complete a trial and receive a water reward, monkeys were required to keep their eyes within a window centered on the target. The window was 1.5°x1.5° during fixation, 3°x3° during smooth target motion, and 5°x5° for 300 ms after an instructive change in target direction. For tests of neural responses to passive visual stimuli, monkeys fixated a small square target centered in an invisible square aperture that was 5° long on each side. The aperture contained 10 dots that moved with 100% coherence at 5°/s in one of the four cardinal directions.

1.3.3 Behavioral paradigms

The direction and temporal tuning of each neuron were characterized in a pre-learning block of pursuit trials where the pursuit target moved at 20°/s in one of 8 possible directions, including all four horizontal and vertical directions and the 45° oblique directions. In some experiments, targets moved in the four cardinal directions with speeds of 5, 10, or 20°/s in different trials.

Each learning experiment consisted of a baseline block and a learning block. During the baseline block (80 to 100 trials), the target moved at 20°/s in one of two opposing cardinal directions, designated the probe (55% of the trials) and control directions (45%). In the learning block, (250 to 300 trials) the pursuit target also initially moved in either the probe (55%) or control (45%) directions; however, targets moving in the probe direction had an 82% chance of adopting a 30°/s orthogonal velocity component at a fixed time after the onset of target motion. The direction and timing of the instructive stimulus were fixed for a given learning block. In some recording sessions, we performed an additional learning experiment after residual behavioral learning had been extinguished with a second baseline block (100-150 trials), or a two-block sequence of learning in the opposite direction (50-100 trials) followed by a baseline block (50 trials). The residual eye velocity measured after the two reversal procedures averaged 27.7% (SD: 30.8%, range: 61.7% to -34.1%) of the original learned response after a baseline block and -1.3% (SD: 16.3%, range: 47.9% to -33.1%) after a learning block in the opposite direction and another baseline block. For 21 neurons, we followed the reversal procedure with a mimic experiment, which consisted of a baseline block followed by a mimic block. The mimic block featured "mimic" trials designed to evoke an eye velocity with the same time course and trajectory as the learned component of eye movement, but without any learning. To prevent learning during the mimic block, mimic trials in the learning direction were counterbalanced by trials that contained the same target perturbation in the opposite direction.

1.3.4 Data analysis

Trials were examined individually by eye to identify the onset and offset times of any saccades; we replaced the intervening eye velocity with a linear interpolation whose endpoints were the eye velocity values at the onset and offset of the saccade. We quantified the magnitude of neural learning in the interval from 100 ms after the onset of target motion to 70 ms after the instruction time, as the difference in mean spike count between the learning trials in the learning block and the probe trials from the baseline block. Neural responses are reported as firing rates, obtained by dividing the spike counts by the duration of the analysis intervals. We verified that all analyses produced similar results if the firing rate changes were converted to Z-scores. Firing rates were smoothed with a 50 ms duration rectangular filter for our figures, but unsmoothed traces were used for quantitative analysis. In the bottom panel of Figure 5B, we took advantage of the larger number of traces to smooth the data with a narrower, 15 ms rectangular filter.

1.4 Results

We recorded from 100 FEF_{SEM} neurons in two monkeys during directional smooth pursuit learning. The neurons we selected for investigation responded vigorously during pursuit prior to learning, and were tuned for the direction of pursuit. In the pre-learning behavioral block, we characterized the direction tuning of each FEF_{SEM} neuron by measuring its mean firing rate during pursuit in each of eight directions spaced 45° apart. The neuron in Figure 1A responded most strongly for pursuit that was upward or obliquely up and left, and therefore had a preferred direction between 90° and 135°. The neuron was only weakly active for purely horizontal pursuit to the right or left.

1.4.1 Behavioral learning

The tuning of the neuron under study specified the direction parameters of the learning experiment (see schematic in Figure 1B). We chose the *learning direction* to be the cardinal direction closest to the neuron's preferred direction: 90° in Figure 1. The cardinal axis orthogonal to the learning direction defined the probe and control directions: 360° and 180° in Figure 1.

Each learning experiment began with a baseline block of trials that used step-ramp target motions in the probe and the control direction to establish the baseline pursuit response prior to learning. After the monkey fixated a stationary central target, the target stepped 2 or 3° in one direction and ramped immediately in the opposite direction at 20°/s

(Figure 1H). For the probe trials in Figure 1F and H, the mean horizontal eye velocity was zero for almost 100 ms after target motion onset, accelerated to the right for 100 to 200 ms, and then approximated the target speed of 20°/s for the remainder of the 750 ms target motion. Vertical target velocity was zero throughout the trial, as was the mean vertical eye velocity prior to learning.

The subsequent learning block introduced learning trials that started like probe trials with a step-ramp of target motion in the probe direction, but underwent a predictable change in target direction at a fixed time. In Figure 1E and G, the initial 20°/s ramp motion took the target to the right. After 250 ms, an upward motion at 30°/s began so that the target moved up and to the right for 500 ms. The direction of the added component of target motion defines the *learning direction*; the 250 ms delay between the onset of target motion and the change in target direction defines the *instruction time*. Both the learning direction and instruction time were fixed for a given learning experiment. Learning trials comprised 45% of the trials in a learning block. The remaining 55% consisted of control trials (45%) and probe trials (10%), which were identical to the control and probe trials in the baseline block.

The average vertical eye velocity from the learning trials (Figure 1E, lower panel, red traces) shows a small upward deflection that starts before the instructive change in target direction and represents the learned response. The initial, early response is followed by a later, more abrupt, “visually-driven” change in eye velocity that is the immediate consequence of the instructive upward target motion. The learned response is not present in the first few learning trials, but grows rapidly and asymptotes after about 20-40 learning trials. This early, upward response reflects behavioral learning because it

1) precedes the onset of the instructive stimulus, and 2) occurs in the infrequent probe trials interspersed in the learning block, even though they lack an instructive change in target motion (Figure 1F, lower panel, blue trace). As reported before, the peak of the learned vertical eye velocity deflection in the probe trials coincides with the instruction time (Medina et al., 2005).

Our learning paradigm elicits robust, but short-term behavioral changes. For any given learning experiment, behavioral learning was quantified as the difference in mean eye velocity between the learning trials and the baseline probe trials, integrated across 100 to 320 ms (Figure 1E, grey shaded region). Integrating eye velocity yields the change in eye position. Behavioral learning averaged 0.8° in Monkey G (SD: 0.2°, range: 0.4° to 1.2°) and 2.1° in Monkey S (SD: 0.7°, range: 0.7° to 4.5°), and was significantly different from zero in all experiments (Mann-Whitney U test: $p<0.001$). Residual behavioral learning did not persist across learning experiments; the mean eye velocity measured in the sessions following training on a particular learning direction was not significantly different from the mean eye velocity in the sessions following learning in the opposite direction (Monkey G: $p= 0.80$, Monkey S: $p=0.88$, Mann-Whitney U test). The rate of behavioral learning also did not vary as the study progressed. Behavioral changes continued to reach a plateau after about 20 to 40 learning trials. We conclude that learning proceeded anew for each experiment, so that we could pool neural data across recording sessions to assess the effect of directional pursuit learning on the activity of the population of neurons in the $\mathrm{FEF}_{\mathrm{SEM}}$.

1.4.2 Neural correlates of learning

The example neuron in Figure 1 produced only a few spikes during the baseline block probe trials (Figure 1D, black raster), because the probe direction was orthogonal to the neuron's preferred direction. During learning trials, the neuron produced the expected vigorous response to the visually-driven eye movement in the learning direction, and also acquired a small learned response that appeared before the instructive change in target direction (Figure 1C, red raster). The learned neural response also appeared in probe trials during the later part of the learning block (Figure 1D, blue raster) and, like the learned eye velocity, began before the time when the instructive change in target direction would have occurred in learning trials.

Different neurons expressed varying degrees of learning. The two neurons whose responses appear in Figure 2 were recorded on different days with strong behavioral learning that reached almost 4°/s by the time of the instructive change in target direction in both experiments (Figure 2 C, D). However, neuron #1 exhibited a large learned change in mean firing rate, while neuron #2 did not. Neuron #2 did respond strongly to the instructive change in target direction, but only after the visual latency of 70 ms typically found in the $\mathrm{FEF}_{\mathrm{SEM}}$ (Figure 2B, red trace; Gottlieb et al., 1994).

The learned change in firing rate, when present, had several important features. First, it appeared in temporal register with the learned change in eye velocity, in the interval preceding the visual input caused by the instructive target motion. Second, it was present in the probe trials in the learning block (Figure 2A, blue trace), and had a transient time course that peaked near the instruction time. Third, it appeared during target motion in a direction that did not evoke much neural activity before learning, as seen by comparison of the blue and black traces in Figure 2A. Therefore, the learned firing rate is related to the acquisition of a vertical response to the horizontal target motion and not to the horizontal eye movement itself, which changed very little as a consequence of learning (Figure 1F, top panel).

Figure 2 shows an important feature of the data that motivated our analysis procedures. The averages of both eye velocity and firing rate followed the same trajectory during learning trials and the interleaved probe trials, up to about 70 ms after the instruction time (Figure 2). Thereafter, the mean eye velocity and firing rate in the learning trials, but not the probe trials, showed large visually-driven reactions to the instructive change in target direction. The sequence of identical responses followed by divergence due to the visual stimulus is expected because the learning and probe trials were interleaved randomly. It allowed us to assess neural changes related purely to learning from the more frequent learning trials in the 220 ms interval from 100 ms after the onset of target motion to 70 ms after the instruction time.

We showed in Figure 2 that the size of the learned response could be very different across FEF_{SEM} neurons even when the concomitant behavioral changes were similar. Only 35% of neurons (15/55 in Monkey G, 20/45 in Monkey S) exhibited a significant learned change in firing rate (Mann-Whitney U test: $p<0.001$). All neurons with statistically significant changes in firing rate showed increases in activity as a result of learning. Because the firing rate in the preceding fixation period almost always remained stable in spite of learning, we argue that the neural changes in the analysis interval probably are due to learning and not to fatigue, decreases in motivation, or recording instabilities. Finally, learning did not affect eye velocity during control trials, and only 5 neurons showed significant changes in firing rate during the control trials from the baseline and learning blocks: 4/55 in Monkey G, 1/45 in Monkey S. Excluding neurons with significant changes in response amplitude during pursuit in the control direction did not alter any of our conclusions.

1.4.3 Neural preference for the instruction time predicts the magnitude of neural learning

Each neuron's response during pursuit of a ramp target motion at constant velocity showed a distinct and repeatable trajectory as a function of time (e.g. Figure 3A). The smoothed firing rate for this $\mathrm{FEF}_{\mathrm{SEM}}$ neuron increased rapidly after the onset of pursuit, peaked approximately 340 ms after the onset of target motion, and declined gradually thereafter. We defined the *neural preference* for a particular time during the pursuit trial as the firing rate at that time normalized for the peak firing rate. At 250 ms after the onset of target motion (intersection of dashed lines), this particular neuron had a neural preference of 0.7, indicating that it fired at 70% of its maximum. The neuron's preferred time was 340 ms after the onset of target motion. We measured neural preference from data acquired in the pre-learning pursuit block, using step-ramp target motion in the direction subsequently chosen to be the learning direction.

The preferred time varied widely across the full sample of $\mathrm{FEF}_{\mathrm{SEM}}$ neurons. In Figure 3B, each row uses color to depict the neural preference for a single $\mathrm{FEF}_{\mathrm{SEM}}$ neuron as a function of time. Neurons are ordered by the latency to 95% of their peak response. The narrowness of the red diagonal band indicates that the time of maximal neural activity is well defined, and its distribution across the full duration of the pursuit movement indicates that the population of $\mathrm{FEF}_{\mathrm{SEM}}$ neurons shows a wide range of preferred times. Thus, individual neurons are most active during limited distinct temporal chunks of the eye movement, only a fraction of the population is close to maximal response at any given time, and the population of FEF_{SEM} neurons encodes all times throughout the entire movement. In our sample, preferred times were fairly evenly distributed across the full pursuit movement duration, with some preponderance of neurons that preferred the initiation of pursuit, from 100 to 200 ms after the onset of target motion (Figure 3C).

Much of the variation in the magnitude of learning across neurons was related to the wide range of neural preferences at the time of the instructive change in target direction. When we plotted the size of the mean learned response in each neuron as a function of its neural preference for the instruction time of 250 ms (Figure 3E), we obtained positive correlations that were statistically significant in both monkeys (Monkey G: $r = 0.50$, $p<0.0001$; Monkey S: $r = 0.58$, $p<0.0001$). Figure 3E uses the mean response averaged across all learning trials as an index of the magnitude of learning, but we obtained similar correlations when we estimated the magnitude of learning from the first or last 40 learning trials within each learning block.

Figure 3E shows the relationship between the neural preference at the single time of 250 ms during pre-learning pursuit and the magnitude of neural learning. For this one time point, the correlation coefficients were quite high. To judge the importance of neural preference at the time of the instructive change in target direction in determining the neuron’s susceptibility to learning, we performed the same analysis shown in Figure 3E, except that we varied systematically the time used to obtain neural preference from 0 to 750 ms relative to the onset of target motion, and computed the correlation between neural preference at each time and the magnitude of neural learning for instructions delivered at 250 ms. For each monkey (Figure 3F), the size of learning across our sample of $\mathrm{FEF}_{\mathrm{SEM}}$ neurons showed the highest correlation with the neural preference near 250 ms, the time of instruction, and lower correlations with neural preference at earlier or later times. Thus, learning with an instruction time of 250 ms engages neurons that specifically prefer 250 ms. The temporally-selective relationship between neural preference and the magnitude of neural learning in Figure 3F provides evidence that the distributed representation of time within the $\mathrm{FEF}_{\mathrm{SEM}}$ may be used to regulate the temporal specificity of pursuit learning.

As an alternate way to examine the relationship between the amount of neural learning in an $\mathrm{FEF}_{\mathrm{SEM}}$ neuron and its temporal preference during pursuit, we plotted the magnitude of neural learning as a function of the difference between the neuron's preferred time and 250 ms (Figure 3D). There is considerable scatter in the plot, but for the population as a whole learning is largest in neurons with preferred times close to 250 ms, and is smaller in neurons with earlier or later preferred times. A small subpopulation of neurons exhibited negative learned responses, but the preferred times of these neurons were evenly distributed before and after the instruction time.

The size of neural learning also was positively correlated with the size of the learned eye velocity and the opponent response of the neuron, defined as the difference in mean firing rate between pre-learning pursuit in the probe direction versus in the learning direction, measured in the interval from 100 to 320 ms after the onset of target motion. Partial correlation analysis (Table 1) revealed that a strong correlation between the magnitude of neural learning and the neural preference for 250 ms persisted even when the correlations with the other variables were taken into account. The size of the opponent response during pre-learning pursuit was not a statistically significant predictor of the magnitude of learning. Not surprisingly, the magnitude of the learned eye velocity was a strong predictor of the magnitude of neural learning in monkey S, who had wider variation in the size of his behavioral learning.

We now ask whether the magnitude of neural learning varies systematically within an individual neuron when we alter the instruction time. The same neuron was exposed to two learning experiments featuring different instruction times associated with disparate neural preferences. The results in Figure 3 predict that the example neuron in Figure 4A should show larger learning for an instruction time of 150 ms, when its neural preference was 1.0, versus an instruction time of 250 ms, when its neural preference was 0.6. The prediction was borne out by performing two different learning experiments with instruction times of 250 and 150 ms, respectively. The amount of neural learning was greater when the instruction time was 150 ms (Figure 4B, top panel), even though the learned change in eye velocity was somewhat larger when the instruction time was 250 ms (Figure 4B, bottom panel).

We studied the activity of 31 neurons (11 in Monkey G, 20 in Monkey S) during two sequential learning experiments that were identical in all respects except the instruction time. The instruction time for one experiment was always 250 ms; the instruction time for the other experiment was chosen amongst 150 ms, 350 ms, or 450 ms. We sorted the 31 neurons into two groups based on whether their neural preference for 250 ms was larger or smaller than for the other instruction time. Then, we computed the size of learning for a 250 ms instruction time minus that for the other instruction time.

These values would be positive or negative depending on whether neural learning was larger or smaller when the instruction occurred at 250 ms.

Neurons with larger preferences for 250 ms showed more learning for an instruction time of 250 ms than for the other instruction time, while neurons with larger preferences for the other instruction time showed less learning for an instruction time of 250 ms, results that were confirmed statistically (Figure 4C, Monkey G: p=0.01; Monkey S: p=0.01; Wilcoxon signed-rank test). The magnitude of neural learning did not depend significantly on alternative explanatory variables, such as the disparity in the sizes of the mean learned behavior elicited by the two instruction times (Monkey G: p=0.76; Monkey S: p=0.88), or the order of presentation of the two instruction times (Monkey G: p=0.24; Monkey S: p=0.28). Finally, the magnitude of neural learning produced with the most frequently used other instruction time, 150 ms, was correlated much better with neural preference for 150 ms (Monkey G: r=0.61, p=0.11, 8 neurons; Monkey S: r=0.75, p=0.001, 15 neurons), than with neural preference for 250 ms (Monkey G: r=0.075; Monkey S: r=0.31).

In conclusion, we have demonstrated that pursuit learning with specific timing requirements selectively engages $\mathrm{FEF_{SEM}}$ neurons that encode the relevant time.

1.4.4 Changes in firing related to learning versus eye movement performance

Do learned changes occur in $\mathrm{FEF_{SEM}}$ neurons because the $\mathrm{FEF_{SEM}}$ plays a direct role in behavioral learning, or simply because learning causes changes in eye velocity to which the $\mathrm{FEF_{SEM}}$ responds? To distinguish between the two scenarios, we presented "mimic" trials in which target motion presented in the absence of learning created an eye movement similar to that produced by learning with an instruction time of 250 ms. During a mimic trial (Figure 5A), a target moving at 20°/s in the probe direction underwent a brief motion in the learning direction. The target motion evoked a mean eye velocity that closely resembled the mean learned eye velocity expressed in the probe trials from the learning block (Figure 5B, top panel). We verified the excellence of the mimicry across neurons using a millisecond-by-millisecond regression analysis of the mimic versus the learned mean eye velocities in the interval from 100 to 320 ms after the onset of target motion. Regression slopes averaged 1.00 across neurons (range: 0.88 to 1.19), and correlation coefficients averaged 0.95 (range: 0.83 to 0.99).

The example neuron in Figure 5 exhibited notably different changes in firing rate as a result of learning versus during the mimic trials (Figure 5B, middle panel), even though the changes in eye velocity were nearly identical. For the 21 neurons from Monkey S that were studied during both learning and the mimic experiment, we quantified the size of the evoked firing rate in the mimic trials as we had for the learning data, in a comparable interval of duration 220 ms (shaded grey region, Figure 5B). We did not find any correlation between the size of the neural responses to the mimic target motion and the learned change in firing rate in the corresponding learning block (Figure 5C, filled circles, $r=0.05$, $p=0.83$)). Some neurons had similar responses in the learning and mimic conditions, while many others had quite different responses. Measuring the sensitivity to eye velocity as the mimic and learned neural responses divided by the magnitude of the corresponding changes in mean eye velocity also failed to reveal a significant correlation ($r=-0.06$; $p=0.78$), reaffirming that minor behavioral differences are unlikely to account for the disparate neural responses.

To control for recording instabilities, we also compared the firing rate during probe trials in the two baseline blocks that preceded the learning and mimic blocks. Most neurons showed very similar responses during the two sets of baseline trials (Figure 5C, open symbols), and plotted along the line of slope one. Finally, to ascertain whether the mismatch between the learned response and the response to mimic target motion originates from the differing visual inputs under the two conditions, we measured the activity of individual neurons during passive, coherent motion of a 5°x5° patch of dots while the monkey fixated a stationary target at the center of the patch. We found no relationship between the size of the disparity between the mimic and learned responses and the neuron's visual sensitivity, computed as the difference in mean firing rate produced by passive dot motion in the learning direction versus in the opposite direction (21 neurons; $r=-0.12$, $p=0.66$).

In contrast to what we found in individual neurons, averaging the responses across the 21 neurons we studied revealed very similar population responses for the mimic and learning conditions (Figure 5B, bottom panel). We conclude that the learned responses of individual neurons in the FEF_{SEM} cannot be thought of solely as secondary consequences of learned changes in smooth eye movement. At least in some neurons, the changes in firing rate are related selectively to an eye movement produced in the context of learning. However, the response of the population is balanced across different behavioral conditions so that the FEF_{SEM} as a whole is always making the same contribution to the smooth eye movement. A similar conclusion has been reached for the cerebellar floccular complex (Kahlon and Lisberger, 2000; Medina and Lisberger, 2009).

Finally, we characterized differences in the temporal preferences of neurons activated by learning versus by the mimic stimulus. For our dataset of 21 neurons, the correlation between neural preference and the size of the learned neural response reached a peak when the neural preference was taken at 250 ms (Figure 6, gray trace), as expected. In contrast, the correlation between neural preference and the size of the mimic response reached a peak for neural preference earlier in the trial (Figure 6, black trace), suggesting that the mimic target motion was most effective for neurons that preferred times during the initiation of pursuit.

1.4.5 Effects of the prior trial on neural and behavioral learning

Previous studies have suggested that motor learning occurs on multiple time scales (Lee and Schweighofer, 2009; Ethier et al., 2008; Smith et al., 2006), including situations where the behavior on a given trial reflects the instruction provided on the previous trial (Yang and Lisberger, 2010). To measure the relative contributions of single-trial versus longer-term learning processes to the behavioral and neural changes reported here, we sorted learning trials based on the identity of the immediately preceding trial. The size of the learned eye velocity was smaller if it had been preceded by a control trial versus by another learning trial. The effect averaged 7.1% and 21.5% in Monkeys S and G and was statistically significant in 15.6% (7/45, Monkey S) and 61.8% (34/55, Monkey G) of the learning experiments in the two monkeys (Mann-Whitney U test, $p<0.05$).

The small trial-over-trial changes in the size of behavioral learning frequently were not present in a similar analysis of the size of neural learning (for example, Figure

7A). In the 35 neurons that showed a significant change in mean firing rate as a result of learning, the trial-over-trial changes in neural learning were distributed fairly evenly above and below zero, and were unrelated to the trial-over-trial learning of eye velocity (Figure 7B). The neural response on learning trials preceded by a control trial were on average 2.1% larger (Monkey S) and 4.4% smaller (Monkey G) than those preceded by another learning trial. Neural response differences were statistically significant in 15.0% (3/20, Monkey S) and 6.7% (1/15, Monkey G) of the neurons (Mann-Whitney U test, $p<0.05$). We conclude that the neural learning in the FEF_{SEM} results from a longer-term process that does not contribute to trial-over-trial changes in the learned behavior.

1.4.6 Nature of temporal information in the FEF_{SEM}

To explore the basis of the temporal responses in the FEF_{SEM}, we used pursuit trials featuring target motion at 5, 10, or 20°/s in the future learning direction to ask whether the activity of individual FEF_{SEM} neurons was most consistent with a representation of speed, elapsed time, or of traversed distance. We collapsed the data across the three speeds and performed regression of firing rate (or normalized firing rate) versus each variable. A regression slope and correlation coefficient of one for any particular variable would indicate that the neuron encodes the value of that variable unambiguously. For the variable of elapsed time, we obtained an average regression slope of 0.90 and correlation coefficient of 0.79 in both monkeys. Slopes and correlations were somewhat smaller for distance (slope=0.62 and 0.61; r=0.75 and 0.71) and for speed (slope=0.67 and 0.66; r=0.65 and 0.62). Thus, the neural responses as a group could encode any of the three variables, but were best related to elapsed time.

1.5 Discussion

For a learned movement to be effective, it not only needs to have the correct trajectory, but must also be produced at the desired time. We have provided evidence that the $\mathrm{FEF}_{\mathrm{SEM}}$ is involved in regulating the timing of learned pursuit eye movements. We show that when driven by a temporally precise instructive stimulus, learned changes in firing rate are preferentially expressed in neurons that respond best at the time of the instructive stimulus during pre-learning step-ramp pursuit. Our results suggest that the $\mathrm{FEF}_{\mathrm{SEM}}$ may be a site where the timing of sensory errors is processed during learning and integrated into appropriate, learned motor commands.

We provide several lines of evidence that the learned responses of neurons in the $\mathrm{FEF}_{\mathrm{SEM}}$ are related selectively to learning, and are not secondary to the altered eye movement. Comparing the changes in firing rate resulting from two different instruction times showed that the magnitude of the learned neural response depended more on the temporal properties of the instructive stimulus than on the size of the learned eye movement. Our analysis of the learned changes in eye velocity and firing rate across single trials revealed a dissociation between the magnitudes of the behavioral and neural responses. Finally, for the same neuron, the change in firing rate associated with a visually-driven eye velocity was often quite different from the change in firing rate produced by learning, even though the visually-evoked eye velocity mimicked the learned eye velocity closely.

1.5.1 Neural mechanisms for temporally selective motor learning

Why should a precisely-timed instructive signal induce learned responses selectively in certain $\mathrm{FEF}_{\mathrm{SEM}}$ neurons, and how might these neural changes give rise to an appropriately timed eye movement? Based on the knowledge that depolarization of the post-synaptic neuron is a key regulator of synaptic plasticity (Malenka and Bear, 2004), we suggest that neurons with a high preference for the instruction time are more susceptible to plasticity than other neurons in the same population because they have higher membrane potentials around the time of the instructive signal. Further, the same neurons presumably receive inputs that are maximally active around the onset of the instruction. The convergence of elevated pre- and post- synaptic activity should favor plasticity in these neurons around the time of the instruction, which in turn will alter the eye movement selectively around the time of the instructive change in target direction.

We cannot answer definitively the question of whether the learned timing of pursuit or neural responses in the $\mathrm{FEF}_{\mathrm{SEM}}$ results from the timing contingencies of the cellular mechanisms of plasticity that are involved, or from timing that emerges out of neural circuit properties. We think it is important to remember that timing is inherent in the responses of neurons in the $\mathrm{FEF}_{\mathrm{SEM}}$ before learning, and that the $\mathrm{FEF}_{\mathrm{SEM}}$ is suited for processing the 250 ms intervals utilized in our learning paradigm because $\mathrm{FEF}_{\mathrm{SEM}}$ neurons track time on the order of hundreds of milliseconds. In contrast, cellular mechanisms such as spike timing-dependent plasticity, in isolation, process intervals on the order of tens of milliseconds (Bi and Poo, 1998). Modeling results indicate that the temporal specificity of order 100 ms in $\mathrm{FEF}_{\mathrm{SEM}}$ responses could emerge and be maintained via network properties (Buonomano, 2005). Thus, we suggest that temporal selectivity in pursuit learning could be the consequence of associative forms of synaptic plasticity acting upon the time-varying pattern of activity created by the properties of the circuit through the $\mathrm{FEF}_{\mathrm{SEM}}$.

1.5.2 Factors contributing to timing signals in the $\mathrm{FEF}_{\mathrm{SEM}}$

A temporally specific encoding of smooth pursuit is unique to the $\mathrm{FEF}_{\mathrm{SEM}}$ and has not been reported in any other locus within the pursuit circuit, including MST (Newsome et al., 1988; Squatrito and Maioli, 1997; Ono and Mustari, 2006), the dorso-lateral pontine nucleus (Ono et al., 2005), and the floccular complex in the cerebellum (Krauzlis and Lisberger, 1994; Lisberger, 2010). Further, the representation of time during smooth pursuit appears to be an inherent feature of the population response in the $\mathrm{FEF}_{\mathrm{SEM}}$ and is present in animals that had never been exposed to a task that requires learned timing (Schoppik et al., 2008).

The motor system has access to both implicit and explicit information about the passage of time (Mauk and Ruiz, 1992; Ivry, 1996; Buonomano and Karmarkar, 2002; Regan and Gray, 2000; Sherk and Fowler, 2001; Caijou et al., 2004; Medina et al., 2005), and is able to rapidly assimilate temporal information to modify behavior. Here, we are using the terms "explicit" and "implicit" to refer to the nature of the signals the brain uses to estimate the duration of a time interval. "Explicit" timing mechanisms would function like a stopwatch, creating a neural state that depends entirely on the number of elapsed milliseconds. "Implicit" mechanisms, on the other hand, would estimate time from less direct cues generated by one's self or the environment. In our learning paradigm, either elapsed time or the distance traveled by the target/eye can be used to cue an upcoming change in target direction (Medina et al., 2005). The $\mathrm{FEF}_{\mathrm{SEM}}$ appears to be an explicit source of temporal information because neural responses during pursuit at three speeds were well correlated with elapsed time, and less so with an implicit measurement such as distance traveled by the eye. Other potential sources of temporal information, such as image motion and eye velocity/acceleration, fail to account for the timed pursuit responses because all are fairly constant during steady state pursuit when the temporal selectivity of $\mathrm{FEF}_{\mathrm{SEM}}$ responses is still clearly present.

1.5.3 Relationship to other sites of pursuit learning

The $\mathrm{FEF}_{\mathrm{SEM}}$ occupies a prime position within the pursuit circuit for mediating motor learning. It receives information that reports discrepancies between the eye and the target via visual motion sensory areas MT and MST (Leichnetz, 1989; Stanton et al., 2005). Lesion and micro-stimulation studies have pinpointed the $\mathrm{FEF}_{\mathrm{SEM}}$ as a major player in regulating the sensory-motor gain for pursuit (Lynch, 1987; MacAvoy et al., 1991; Tanaka and Lisberger, 2001), a mechanism that could determine what gets learned, and how well. Finally, the $\mathrm{FEF}_{\mathrm{SEM}}$ is strongly connected to the caudate nucleus (Cui et al., 2003), an area involved in assessing reward contingencies, which could be used to guide motor learning.

A previous study in the $\mathrm{FEF}_{\mathrm{SEM}}$ failed to uncover a consistent expression of neural learning using a training procedure that provided a change in target speed 150 ms after the onset of target motion in the learning direction (Chou and Lisberger, 2004). There are two possible reasons for the discrepancy between this earlier finding and our present results. First, behavioral learning is larger and more consistent for changes in target direction than target speed (compare results presented here with Kahlon and

Lisberger, 1996). Thus, the direction-learning paradigm may induce more persuasive neural changes than the speed learning paradigm, as has been found in the cerebellar flocculus (compare Medina and Lisberger, 2008, 2009 with Kahlon and Lisberger, 2000). Second, the recordings during speed learning did not examine how learned FEF_{SEM} responses varied as a function of neural preference for the time of the instructive stimulus. The instructive change in target speed occurred 150 ms after the onset of target motion, implying that learning should be expressed mainly in neurons that respond most strongly at the initiation of pursuit. Averaging across neurons having a range of temporal preferences would dilute any learning-related effects. Consistent with this explanation, a subpopulation of FEF_{SEM} neurons did exhibit significant changes in firing rate during speed learning (Chou and Lisberger, 2004).

The cerebellar flocculus, several synapses downstream of the FEF_{SEM}, also may play a causal role in temporally specific pursuit learning. Purkinje cells show changes in simple spike activity around the time of the instructive stimulus during learning in both the OFF and ON directions of the Purkinje cell under study (Medina and Lisberger, 2008, 2009). In one model of the cerebellar microcircuit, a sparse representation of time in the granule cell population provides the excitatory drive for Purkinje cells. Different granule cells would provide inputs to Purkinje cells at different times during a movement so that visually-driven climbing fiber inputs could potentiate or depress the granule-Purkinje synapses that were active 100 ms prior to the arrival of the climbing fiber signal (Buonomano and Mauk, 1994). Thus, the cerebellum could act independently in learning motor timing, or inputs from the FEF_{SEM} could contribute to the temporal sparseness of the granule cell population in a way that is enhanced by learning in the FEF_{SEM}. Recent work also has highlighted the possibility that learning occurs on different time scales (Lee and Schweighofer, 2009; Ethier et al., 2008; Smith et al., 2006; Yang and Lisberger, 2010) with the possibility of very rapid short term learning in the cerebellar cortex as a prelude to slower, longer-term changes in the FEF_{SEM}.

1.5.4 Utility of a high-dimensional motor code

Neurophysiological studies of motor and perceptual learning reveal a common theme: changes are localized to neurons whose properties best capture the features of the training stimulus (Arce et al., 2010; Paz et al., 2003; Recanzone et al., 1993; Schoups et al., 2001; Yang and Maunsell, 2004). In real life, the learning rule can be very complex. Thus, the dimensionality of the neural representation of movements limits the flexibility of the motor system in terms of what can be learned quickly. For many years, it was commonly believed that the responses of motor cortex neurons could be modeled by a time-invariant combination of limb kinematics and dynamics (Evarts, 1968; Georgopoulos et al., 1982; Moran and Schwartz, 1999). Recently, examination of a broader population of neurons in the primary motor cortex (M1), dorsal premotor cortex (PMd), and the FEF_{SEM} has revealed considerable heterogeneity in movement-related neural responses (Hatsopoulos et al., 2007; Churchland and Shenoy, 2007). Many response patterns are explained poorly using standard movement parameters such as acceleration, speed, and direction. We propose that the FEF_{SEM} and other motor cortices are important for facilitating action selection. The FEF_{SEM} encodes smooth pursuit movements flexibly along seemingly baroque but perhaps behaviorally relevant dimensions, such as time, so that error and reward signals can act selectively on a sub-region within the movement space to drive rapid, precise motor learning.

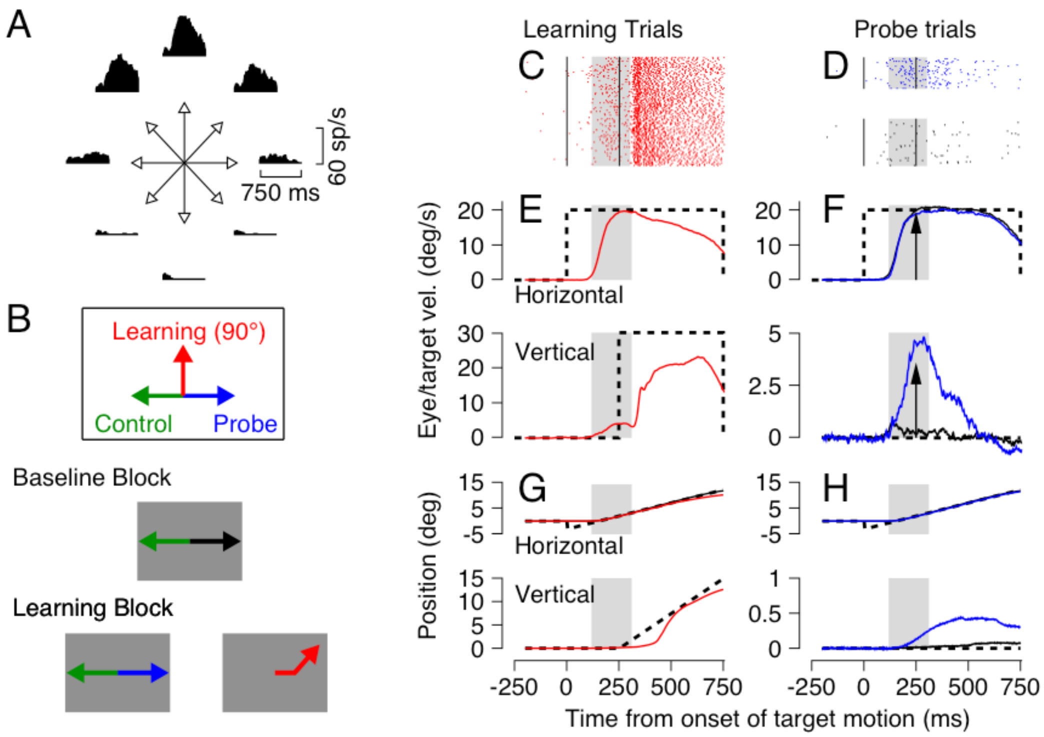

Figure 1.1: Expression of learning in the FEF$_{SEM}$.

(A) The direction tuning of an example neuron. (B) Top: The control (180°), probe (360°) and learning (90°) directions chosen for the neuron in A. Bottom: a cartoon of the trial configurations for the baseline block and the subsequent learning block. (C-G) Example of neural and behavioral responses measured during learning trials. (D-H) Comparison of neural and behavioral responses from probe trials in the learning block (blue) with probe trials in the baseline block (black). (C, D) Raster of spikes emitted during all trials: the top row corresponds to the last trial. (E, F) mean horizontal and vertical eye velocity. (G, H) mean horizontal and vertical eye position. The black dashed trace depicts motion of the pursuit target, the grey shading shows the analysis interval, and the black arrow at 250 ms denotes the instruction time.

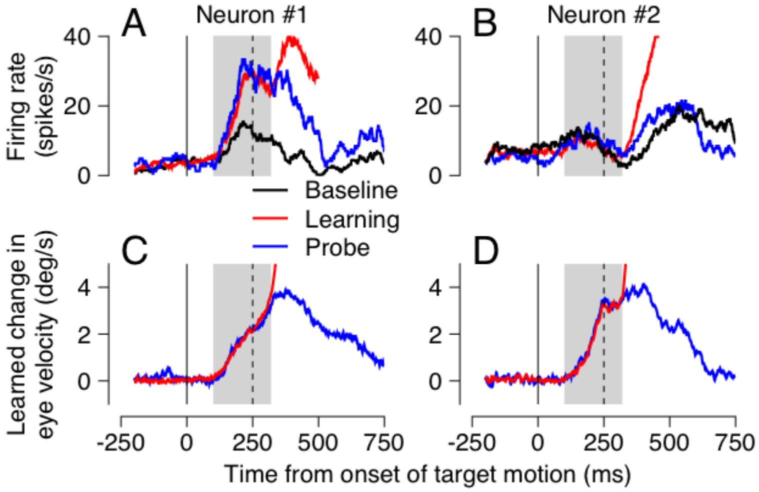

Figure 1.2: Expression of pursuit learning in two example FEF$_{SEM}$ neurons.

Mean firing rates (A,B) and changes in eye velocity (C,D) as a function of time from the onset of target motion. The vertical dashed lines show the time of the instructive change in target direction. Black, blue, and red traces show data obtained respectively during probe trials in the baseline block, probe trials in the learning block, and learning trials. The grey shading indicates the analysis interval from 150 ms before to 70 ms after the time of the change in target direction.

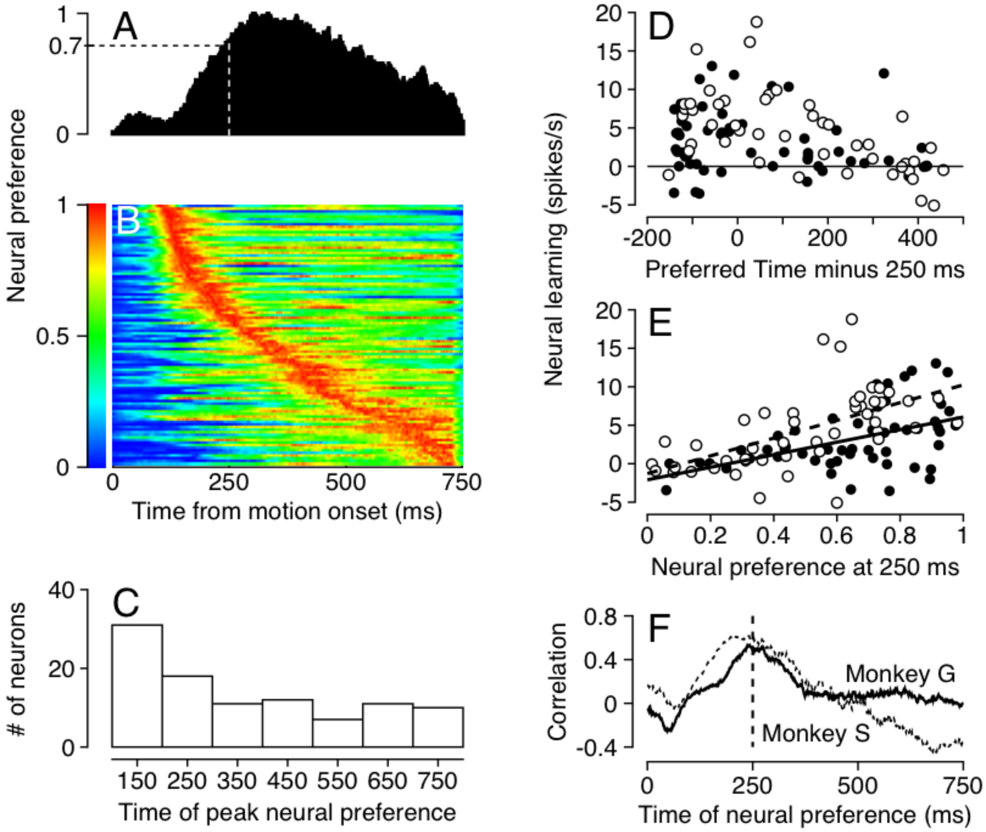
A
B
C
D
E
F
Neural preference
1
0.7
0
1
0.5
0
0
250
500
750
Time from motion onset (ms)
# of neurons
40
20
0
150
250
350
450
550
650
750
Time of peak neural preference
Neural learning (spikes/s)
20
15
10
5
0
-5
-200
0
200
400
Preferred Time minus 250 ms
0
0.2
0.4
0.6
0.8
1
Neural preference at 250 ms
Correlation
0.8
0.4
0
-0.4
Monkey G
Monkey S
Time of neural preference (ms)

Figure 1.3: Relationship between the size of neural learning and neural preference for the instruction time of 250 ms.

(A) Example of neural preference as a function of time from target motion onset. The neuron's preference for 250 ms is specified by the intersection of the vertical and horizontal dashed lines. (B) Summary of neural preference during pre-learning pursuit for all 100 FEF_{SEM} neurons in our sample, sorted by the time when neural preference first reaches 0.95. Each horizontal line of the color map shows the preference of one neuron as a function of time; neural preference is quantified by the pixel color. (C) Distribution of times of maximal neural preference. (D) The size of neural learning is plotted as a function of the neuron's preferred time minus 250 ms. (E) The size of neural learning is plotted as a function of the neural preference for 250 ms. The lines show linear regression fits to the data from each of the two monkeys. In D and E, each symbol shows data for one neuron, and filled versus open symbols show data from the two monkeys. (F) Correlations across neurons between the size of neural learning and the neural preference as a function of the time used to assess neural preference. The two traces show results from the two monkeys. The vertical dashed line indicates the time of the instructive change in target direction, 250 ms after the onset of target motion.

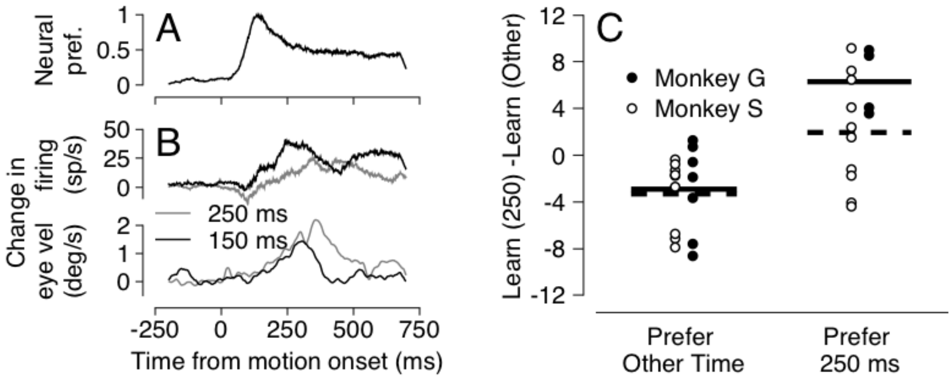

Figure 1.4: Effect of the instruction time on the magnitude of the learned neural response.

(A) Neural preference as a function of time for an example neuron. (B) Baseline-subtracted mean firing rate (top panel) and eye velocity (bottom panel) when the same neuron underwent learning using an instruction time of 250 ms (grey trace) or 150 ms (black trace). (C) Each symbol plots data from a single neuron (n=31). Each neuron is sorted into one of two x-axis groups according to whether its neural preference was greater for 250 ms or for the other instruction time used in the experiment. The y-axis plots the size of the neural learning for an instruction time of 250 ms minus the size of the neural learning for the other instruction time. The horizontal lines indicate the group means. Filled versus open symbols and different line styles indicate data for the two monkeys.

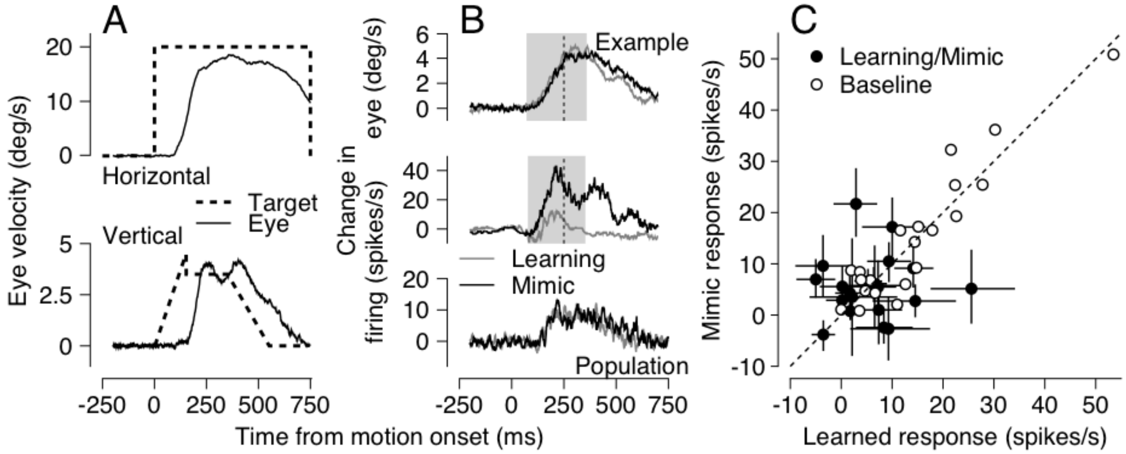

Figure 1.5: Assessment of whether learned changes in neural firing can be attributed solely to changes in eye movement performance.

(A) The dashed and continuous traces show target and eye velocity during a tracking that mimicked the trajectory of the learned eye velocity measured from probe trials in the learning block. (B) Black traces show data from the mimic trials and grey traces show the learned responses. Top panel: averages of eye velocity. Middle panel: average firing rates for the example neuron. Bottom panel: the population responses, averaged across all neurons. (C) Filled symbols compare learned firing rates with mimic responses for the full sample of neurons. Open circles compare the responses from the probe trials in the baseline blocks preceding the learning or the mimic experiments. Error bars denote 95% confidence intervals. The dashed line has a slope of one.

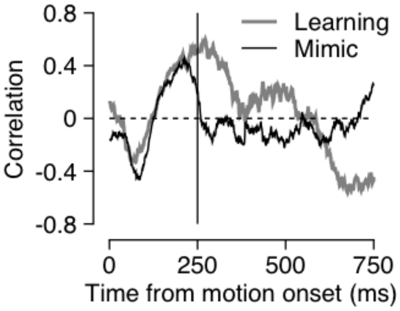

Figure 1.6: Time course of correlation between neural preference and size of learned and mimic responses.

Correlations between neural preferences at the times on the x-axis and the learned response with an instruction time of 250 ms (grey trace), or the mimic response (black trace). Results reflect all 21 FEF_{SEM} neurons studied in the mimic experiments.

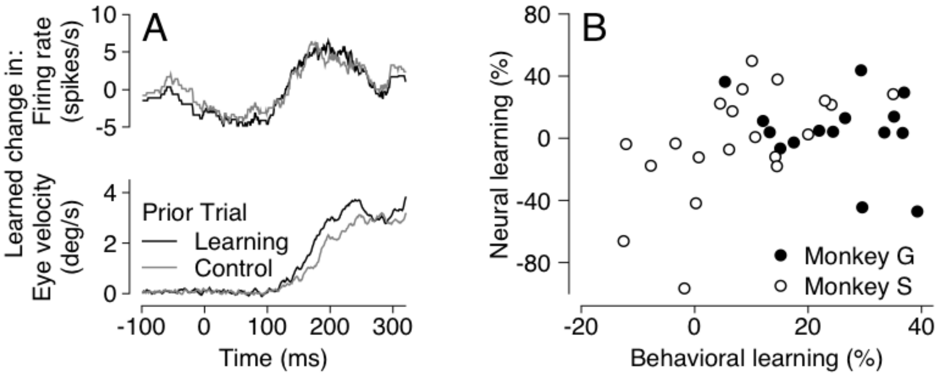

Figure 1.7: Trial-over-trial effects on learned eye velocity and firing rate.

(A) Example from a single experiment of baseline-subtracted mean firing rate (top panel) and eye velocity (bottom panel) from learning trials preceded by a control trial versus by another learning trial. (B) Population analysis: each symbol shows data from an individual neuron and open versus filled symbols show data from the two monkeys.

	MONKEY G		MONKEY S	
	Correlation, significance	Mean [range]	Correlation, significance	Mean [range]
Neural preference for 250 ms	0.43 p=0.001	0.63 [0.06 to 0.98]	0.36 p=0.02	0.50 [0.01 to 0.98]
Opponent firing rate	0.22 p=0.11	19.2 spikes/s [0.6 to 88.7]	0.27 p=0.08	19.0 spikes/s [-1.9 to 77.1]
Behavioral learning	0.18 p=0.19	0.8 degrees [0.4 to 1.2]	0.47 p=0.01	2.1 degrees [0.7 to 4.5]

Table 1.1: Partial correlation coefficients between the magnitude of neural learning and other neural or behavioral parameters.

For assistance in interpreting the correlations, the table also shows the mean and range of each variable in the two monkeys.

Chapter 2

Dynamics of frontal eye field and cerebellar activity during smooth pursuit learning

2.1 Abstract

Smooth pursuit learning elicits changes in the responses of neurons in the smooth eye movement region of the frontal eye fields (FEF_{SEM}), a motor cortex for pursuit, and in the floccular complex, a cerebellar locus for pursuit. To better understand the respective roles of the two structures in pursuit learning, we compared how their representations of learning emerged and evolved across movements as the monkey acquired and practiced a precisely-timed smooth eye movement. The two population averages, along with the learned behavior, all had very similar learning dynamics. However, the learning dynamics of individual neurons were heterogeneous, and differed between the two brain areas. Proportionally more neurons in the floccular complex acquired learning at the same rate as the behavior. Further, floccular complex neurons active early in the learning process tended to maintain elevated responses throughout learning, while learned responses in the FEF_{SEM} were more likely to decrement substantially with further practice. Finally, the millisecond-by-millisecond time course of the mean learned responses in the floccular complex were fairly stereotyped and resembled that of the

mean learned eye velocity; while the responses of different FEF_{SEM} neurons peaked at unique times during the learned eye movement. We conclude that pursuit learning arises from multiple neural components that emerge at different rates, and that the FEF_{SEM} and the floccular complex serve at least partially distinct functions during learning.

2.2 Introduction

The nervous system can use sensory reports of the errors that occur during one movement to improve the accuracy of subsequent movements, a process commonly referred to as motor learning. Motor learning is dynamic by nature; behavioral improvements occur in increments, and the increments become smaller with practice. Nevertheless, traditional approaches to understanding the neural basis of motor learning have largely focused on a comparison of the average neural activity before and after learning, without considering the dynamical aspect of the learning process. Tracking the evolution of neural activity while an animal acquires a learned movement can provide insight into the neural mechanisms that underlie motor learning, while a comparison of the learning dynamics from multiple locations throughout the neural circuit may shed light their respective contributions to the learning process.

Primates presented with a small object moving across their visual field can initiate an ocular tracking behavior known as smooth pursuit eye movements. Pursuit provides an excellent opportunity for exploring the neural basis of motor learning. Reliable learning can be induced in pursuit learning by repeatedly delivering a given change in the direction of motion of the visual target at a predictable time (Medina et al., 2005). The learned changes in the behavior accrue rapidly and plateau within a few dozen movements. Thus, it is possible to make a detailed comparison between changes in the behavioral and neural responses throughout the learning process. In addition, the neural circuit for smooth pursuit has been extensively characterized. As in many other types of movements, both the motor cortex (Keating, 1991; MacAvoy, et al., 1991) and the cerebellum (Westheimer and Blair, 1973; Rambold et al., 2002) are necessary for the proper production of smooth pursuit. Portions of the motor cortex and the cerebellum dedicated to smooth pursuit include, respectively, the smooth pursuit region of the frontal eye fields (FEF_{SEM}) and the floccular complex. The FEF_{SEM}, which receives information about visual motion from sensory areas MT and MST (Leichnetz, 1989; Stanton et al., 2005), plays a key role in setting the gain of visual-motor transmission, or the extent to which the motor command is altered by incoming visual signals (Tanaka and Lisberger, 2001, 2002). The floccular complex is situated closer to the output of the pursuit circuit, and encodes the dynamics of the eye movement (Shidara et al., 1993; Krauzlis and Lisberger, 1994).

Despite their differing functions in pursuit, both FEF_{SEM} neurons (Li and Lisberger, 2011) and Purkinje cells in the floccular complex (Medina and Lisberger, 2008) exhibit changes in mean firing rate as a result of learning. Now, we have tested the hypothesis that the FEF_{SEM} and the floccular complex have distinct roles in pursuit learning by comparing how activity in the FEF_{SEM} and the floccular complex change throughout the learning session, in relation to the accompanying changes in the learned behavior. Our results suggest that pursuit learning is composed of multiple adaptive neural processes with diverse dynamical properties, and that these processes are engaged differently in the FEF_{SEM} and the floccular complex, possibly to drive separate aspects of pursuit learning.

2.3 Materials and Methods

2.3.1 General methods

We report further analysis of two sets of data that have been published previously to address different questions (Medina and Lisberger, 2008, 2009; Li and Lisberger, 2011). Data were recorded from four adult male rhesus monkeys during a paradigm that induced directional learning in smooth pursuit eye movements. Two monkeys participated in recordings from the FEF_{SEM} and two in recordings from Purkinje cells in the floccular complex of the cerebellum. The experimental protocol for the two brain areas used the same general procedures and learning paradigm, with minor differences in technique that will be mentioned at the relevant places in the following sections.

Throughout each daily experiment, the monkey sat comfortably in a primate chair with his head held stationary using implanted hardware. We monitored eye position using a magnetic scleral search coil system (Ramachandran and Lisberger, 2005). The hardware for fixing the head, the eye coil, and the recording chamber were attached in sterile surgery with the monkey under isofluorane anesthesia. Post-surgical discomfort was mitigated by several days of treatment with opiate and non-steroidal analgesics. The experimental procedures and protocols were approved in advance by the *Institutional Animal Care and Use Committee* of the University of California, San Francisco, and were in accordance with the *National Institutes of Health Guide for the Care and Use of Laboratory Animals*.

2.3.2 Experimental design

Experiments took place in a dimly lit room. Target presentation was different for the two brain areas, but the resulting learning was essentially identical. For recordings from the FEF_{SEM}, visual targets were presented on a BARCO monitor (model number: CCID 7651 MkII) that was placed 40 cm in front of the eye and subtended 61x42° of visual field. For recordings from the floccular complex, visual targets were created by imaging the light from a projector. The beam was deflected and moved using a mirror-galvanometer system, and was projected onto the back of a projection screen that was located 30 cm in front of the monkey and subtended 53x53° of visual field.

Visual stimuli were presented in a series of individual trials. Each trial started when the monkey fixated a 0.5° white spot at the center of the screen for 500 to 1000 ms. Subsequently, the target underwent a step displacement followed by a ramp motion that lasted 750 ms. Finally, the target stopped at its final position for an additional 500 ms. Throughout the trial, monkeys were required to keep their gaze within a small window centered on the target. The size of the fixation window varied slightly between the recordings from the two structures (see Medina and Lisberger, 2008; Li and Lisberger, 2011). Failure to fulfill the eye position requirements resulted in immediate termination of the trial. At the end of each successfully completed trial, the animal received a small drop of water or juice.

Each learning experiment consisted of a characterization of the direction tuning of the neuron under study (~100 to 150 trials), a baseline block to establish the detailed responses of the neuron before learning (~100 trials), and a learning block (~250-300 trials). We describe the experimental design for recordings from the $\mathrm{FEF_{SEM}}$ first, and then list the minor differences for the floccular complex recordings. The pre-learning characterization block delivered 10 to 20 repetitions of step-ramp target motion at 20°/s in each of the eight cardinal and oblique directions (Figure 1A). During the subsequent baseline block, the target moved at 20°/s along the cardinal axis closest to orthogonal to the preferred direction of the neuron under study. The example neuron that provided the data illustrated in Figure 1A preferred upward pursuit, so the axis for the baseline block was horizontal (Figure 1B). One direction along the baseline axis was designated as the probe direction (black arrow) and the other as the control direction (blue arrow). 55% of the baseline trials were "probe" trials and 45% were "control" trials, named thusly because they featured target motion in the probe or in the control direction. In the learning block, we introduced "learning" trials that provided an instructive stimulus for a learned change in the direction of pursuit (after Medina et al., 2005). In each learning trial, the target initially moved in the probe direction at 20˚/s; 250 ms after the onset of target motion, the target adopted a 30˚/s velocity component in the learning direction (Figure 1C, second row of icons). Learning trials comprised 45% of the total number of trials in the learning block for recordings from the $\mathrm{FEF_{SEM}}$, probe trials comprised 10%, and control trials comprised 45%. In all blocks, the different types of trials were interleaved in random order.

There were a few minor differences between the experimental design for the floccular complex recordings, versus that described above for the FEF_{SEM}. First, the pre-learning characterization block also served as the baseline block; as a result, only 12.5% of the trials in the baseline block featured target motion in the probe direction. Second, the learning block did not include target motion in the control direction, so that learning trials comprised 90% of the trials in the learning block and probe trials provided the other 10%. The schematics in Figure 1C summarize the differences in experimental design for the recordings from the two brain areas.

2.3.3 Data acquisition

Horizontal and vertical eye position were sampled at 1 kHz and passed through analog differentiators with a cutoff of 25 Hz to yield the eye velocity traces. The eye velocity traces from each trial were examined on a computer screen to identify and excise any saccades, which were replaced by a linear interpolation whose endpoints were the eye velocity values at the onset and the offset of the saccade.

Single-unit recordings from the FEF_{SEM} and the floccular complex were made, respectively, using quartz shielded tungsten electrodes from Thomas Inc., and glass shielded platinum-iridium microelectrodes manufactured in our laboratory. FEF_{SEM} neurons were characterized by robust, directionally tuned activity during smooth pursuit, and weak or non-existent responses to saccades, visual motion, or eye position, while Purkinje cells in the floccular complex were identified based on their modulation to sinusoidal pursuit and the presence of complex spikes. The recorded voltage signals were amplified, filtered, and sorted offline into discrete units using methods described in detail elsewhere (Medina and Lisberger, 2008; Li and Lisberger, 2011). For the analyses reported here, sorted waveforms were converted into spike trains with a temporal precision of 1 ms.

2.3.4 Generation of neural and behavioral learning curves

Although all learning experiments produced statistically significant changes in eye velocity (significance level $p<0.001$; Mann-Whitney U test), expression of neural learning was highly variable across the FEF_{SEM}, and to a lesser extent, the floccular complex. Thus, the preliminary step was to identify neurons with significant expressions of learning, so as to generate learning curves exclusively from these neurons.

We used three different methods to identify neurons with significant expressions of learning, all of which produced largely overlapping sets of neurons. All three methods compared neural responses from the complete set of probe trials in the baseline block with the first 100 learning trials from the learning block. First, we included neurons with a significant change in mean spike count, integrated across in the interval spanning 100 to 320 ms after the onset of target motion, between the baseline block probe trials and the learning trials (significance level $p<0.01$; Mann-Whitney U test). This method identified 37/86 FEF_{SEM} neurons and 22/31 Purkinje cells. Second, we screened for neurons that showed a significant change in neural responses that was present only transiently during the block of learning trials. For each neuron, we determined whether learning caused an increase or decrease in the mean spike count (integrated across 100 to 320 ms), counted the number of learning trials whose spike count lay above the 95th percentile (for an increase in mean spike count) or below the 5th percentile (for a decrease) of the spike count distribution from the baseline block probe trials, and included neurons with at least 11 such learning trials (1% chance occurrence). 9/86 FEF_{SEM} neurons and 2/31 Purkinje cells were added to the group of neurons for further study using the second method. Finally, to screen for neurons with learned responses that are brief in time during each individual trial, we smoothed the 0 to 320 ms portion of the spike train of each trial with a 50 ms rectangular filter, performed a millisecond-by-millisecond statistical comparison of the smoothed responses from the learning trials with those from the baseline block probe trials, and included all neurons with at least 50 time points where the two populations were significantly different (significance level $p<0.01$; Mann-Whitney U test). 2/86 FEF_{SEM} neurons and 0/31 Purkinje cells were added to the group of neurons for further study using the third method. In total, 48/86 FEF_{SEM} neurons and 24/31 Purkinje cells satisfied at least one of the three criteria.

We used an adaptive algorithm that has been described in detail elsewhere to generate a smoothed estimate of the activity of each neuron during learning (Brown et al., 2000; Frank et al., 2002; Wirth et al., 2003).

In brief, the algorithm models the underlying firing rate of the neuron, $\lambda(t \mid \theta)$, on each trial as a cardinal spline with 39 control points, $\{\theta_j\}_{j=1}^{39}$, located at 20 ms intervals, $\{t_j\}_{j=1}^{39}$, from -100 ms to 660 ms relative to the onset of target motion:

$$\lambda(t \mid \theta) = \begin{bmatrix} v(t)^3 & v(t)^2 & v(t) & 1 \end{bmatrix} \begin{bmatrix} -0.5 & 1.5 & -1.5 & 0.5 \\ 1 & -2.5 & 2 & -0.5 \\ -0.5 & 0 & 0.5 & 0 \\ 0 & 1 & 0 & 0 \end{bmatrix} \begin{bmatrix} \theta_{j-1} \\ \theta_j \\ \theta_{j+1} \\ \theta_{j+2} \end{bmatrix}, \qquad (1.1)$$

where $t \in (t_j, t_{j+1}]$, $v(t) = \dfrac{t - t_j}{t_{j+1} - t_j}$, and $\lambda(t \mid \theta) = \max(\lambda(t \mid \theta), 0)$ to ensure a positive firing rate. At each millisecond, t, the algorithm updates the four nearest control points based on the difference between the firing rate function specified by the current values of the control points, $\lambda(t \mid \theta_{t-1})$, and the actual value of the raw spike train, $dN(t)$, where a spike is 1, a pause is 0, and θ_t is the vector of control points at time t:

$$\theta_t = \theta_{t-1} + \varepsilon \frac{d\lambda}{d\theta}\left[dN(t) - \lambda(t \mid \theta_{t-1})\right] , \qquad (1.2)$$

At the end of each trial, the updated control points serve as the initial template for the next trial. The learning rate of the algorithm, ε, which we fixed at 0.005 (5 Hz), determines the extent to which the new information from the spike train modifies the existing control points. Our conclusions were not dependent on the exact parameters chosen for the algorithm, as comparable results were produced using learning rates of 0.01 or 0.0025 and a 10 or 50 ms spacing between successive control points.

The first step in the procedure to estimate the firing rate of a given neuron on each trial was to construct a matrix of raw spike trains from the full set of baseline block probe trials and learning trials. Each row in the matrix was the spike train from a single trial spanning 200 ms before to 750 ms after the onset of target motion, and the first row contained data from the earliest probe trial presented in the baseline block. The algorithm represented by Equations (1.1) and (1.2) was run once forward in time, starting with the earliest probe trial in the baseline block, and once in reverse, starting with the last learning trial. When the algorithm was run forward in time, the control points were initialized from the mean firing rate from all probe trials in the baseline block. When the algorithm was run in reverse, the control points were initialized from the mean firing rate from the last 20 learning trials. Running the algorithm forward and in reverse produced two firing rate estimates for each trial, which were then averaged to yield the final firing rate estimate for that trial (examples shown in Figure 2D).

To smooth the behavioral responses, we organized the raw eye velocity traces from the baseline block probe trials and the learning trials in the manner described above for the spike trains, and then convolved each millisecond of data across trials with an exponential filter whose decay constant was chosen to be -0.077 to match the parameters used for the adaptive algorithm. As with the neural data, the behavioral data were smoothed forward and backward in time, and the results were averaged. We did not use the exponential filter to smooth the neural data because the results from the adaptive algorithm were less noisy; however, we confirmed that our general conclusions were unchanged when spike trains were smoothed with an exponential filter.

The learning curves quantified the magnitude of the neural or behavioral response as a function of the trial number. Each learning curve included data from last 9 probe trials in the baseline block, followed by data from the first 100 learning trials. To ensure that learning curves exclusively featured responses associated with learning, we focused the interval spanning 100 to 320 ms after the onset of target motion, because inherent delays within the pursuit circuit prevented the instructive change in target direction at 250 ms from directly affecting neural and behavioral responses until at least 70 ms later, at 320 ms. Therefore, we measured the behavioral response on each trial as the integral of the smoothed eye velocity trace from 100 to 320 ms; for the neural responses, the firing rate estimate was integrated from 100 to 300 ms to account for the ~20 ms resolution of the adaptive algorithm. Finally, we subtracted the average of the 9 baseline values from each point along the learning curve, and normalized the resulting curve by its most extreme value so that all learning curves had a maximal value of 1.

2.4 Results

In recordings from both the FEF_{SEM} and the floccular complex, we searched for neurons that responded selectively during smooth pursuit, and characterized responsive neurons according to their preferred direction during step-ramp target motion (Rashbass, 1961). We defined the preferred direction as the direction of target motion that elicited the largest mean firing rate, which was upward, or 90°, for the example neuron in Figure 1A.

As described in the Materials and Methods, we chose the learning direction to be the cardinal direction closest to the neuron's preferred direction, and the probe direction to be orthogonal to the learning direction. For the neuron used to create Figure 1, target motion in the learning trials started in the rightward probe direction and then added a component of motion in the upward learning direction. Repeated exposure to the instructive target motion elicited learned upward changes in the mean vertical eye velocity that appeared before the instructive motion (see arrow in Figure 1D, bottom), but minimal concurrent changes in the mean horizontal eye velocity (Figure 1D, top).

Our goal in the present paper differs from those in our prior reports, which documented how mean eye velocity and firing rate changed as a result of directional pursuit learning (Medina and Lisberger, 2008, 2009; Li and Lisberger, 2011). Here, we treated learning as a dynamic process and evaluated how eye velocity and firing rate evolved across learning trials. Thus, results are typically presented as a function of the number of the learning trial during the learning block. Because the monkey paces the experiment, absolute time is not under our control. We return to a conventional analysis of the mean learned firing rate and eye velocity as functions of time during single pursuit responses only in the final figure of the paper.

Learned eye velocities emerged gradually over the course of a learning session. In each learning trial, the target started to move to the right at time zero, and underwent an "instructive" change in direction 250 ms later. During the first few learning trials (Figure 2A, top blue traces), before any learning had occurred, the vertical eye velocity remained near zero until about 70 ms after the change in target direction. At that time, the vertical eye velocity exhibited a sharp upward deflection that we will refer to as the visually-guided eye movement because it was driven by the change in target direction. As we proceeded from 1st to the 20th learning trial in Figure 2A, the general size and shape of the large visually-guided eye movement were unaffected, but the eye velocity acquired an earlier upward deflection that peaked around the time of the change in target direction, 250 ms after rightward motion onset. This deflection in vertical eye velocity became progressively larger in later-occurring learning trials, and appeared too early to be part of the visually-guided response. Therefore, the early upward eye velocity response is understood best as a learned response, rather than as a visually-guided response or random eye velocity fluctuations.

Learned changes in firing rate also emerged gradually over the course of a learning session. Prior to learning, neurons showed little or no firing during baseline probe trials that took the pursuit target and the eyes exclusively in a direction that was approximately orthogonal to the neuron's preferred direction (Figure 2A, black raster). In the first learning trial (first row, red raster), the neuron retained a low level of activity up to 320 ms, 70 ms after the change in target direction. Thereafter, it started to fire vigorously because the change in target direction evoked an eye velocity in a direction close to the preferred direction of the neuron. Across learning trials, the neural response during the visually-guided eye movement did not change in size, but a small learned response developed in the interval between the onset of rightward target motion and the change in the direction of target motion.

The data in Figures 2A and C are raw and unsmoothed. Figures 2B and D show that the same effects persisted after analyses that smoothed the data (see Materials and Methods). As the sessions proceeded from the 1st to the 20th learning trial, both the smoothed eye velocity and firing rate traces showed a gradual acquisition of learned responses that preceded the onset of the instructive change in target direction.

2.4.1 Relationship between neural and behavioral learning dynamics

We used learning curves, which measure the size of the learned change in spike count or eye position as a function of the number of learning trials, to portray the learning dynamics of individual neurons and of the behavior (see Materials and Methods). Figure

3A plots the neural (red traces) and behavioral (blue traces) learning curves for eight different recording experiments, four each from the $\mathrm{FEF_{SEM}}$ and the floccular complex. Neural learning curves from both brain areas often diverged considerably from the behavioral learning curves, suggesting that the learning dynamics of individual neurons in the $\mathrm{FEF_{SEM}}$ and the floccular complex do not merely reflect changes in the animal's motor performance across learning trials. Further, the shape of the behavioral learning curve was fairly stereotyped across experiments, consisting of a brief acquisition period where the size of the learned behavior increased rapidly, followed by an extended maintenance period where the size of the learned behavior gradually stabilized, while the shapes of the neural learning curves were much more heterogeneous.

Although the learning curves of individual neurons sometimes bore little resemblance to the behavioral learning curve, it was possible to recover the behavioral learning curve by averaging across neurons. Figure 3B reveals a high degree of similarity between the mean behavioral learning curve (Figure 3B, blue traces) and the average of the full set of learning curves from either the $\mathrm{FEF_{SEM}}$ or the floccular complex (Figure 3B, red traces). To determine the minimum number of neurons from either brain area needed to produce an average population learning curve that faithfully tracked the behavioral changes, we randomly drew neurons (with replacement) from the original $\mathrm{FEF_{SEM}}$ and floccular complex datasets to generate pools containing anywhere between one neuron and the total number of neurons present in each of our original datasets. We drew 1000 pools of each size, and quantified the performance of each pool by measuring the amount of variance in the behavioral learning curve that could be explained by the mean population learning curve. Single neurons from both the $\mathrm{FEF_{SEM}}$ and the floccular complex were variable in their ability to faithfully track the behavioral changes, and accounted for, on average, 60.5 and 50.9% of the variance in the behavioral learning curve, with no significant difference between the two brain areas ($p=0.23$; Mann-Whitney U test). Performance improved rapidly as a function of pool size. A pool of as few as 10 randomly selected neurons from the floccular complex or the FEF_{SEM} accounted for, on average, nearly 90% of the variance in the behavioral learning curve. Overall, the performances of the two brain areas were extremely similar across all pool sizes, indicating that the FEF_{SEM} and the floccular complex encode equally well the time course of the changes in eye velocity during the learning process.

2.4.2 Comparison of learning dynamics in the FEF_{SEM} and the floccular complex

The example learning curves in Figure 3A suggest that learning in the behavior can either lead or lag learning in individual neurons from either the FEF_{SEM} or the floccular complex. To compare and contrast the rates at which the two brain areas acquired learning, we defined the “trial of learning acquisition” for each neuron as the trial on which its learning curve first reached 75% of maximum. We then plotted the trial of acquisition for neural learning as a function of the trial of acquisition for behavioral learning, defined by the same threshold from the behavioral results for the same experiment (Figure 4A). Neurons that plot on the oblique dashed line showed identical trials of acquisition for neural and behavioral learning, while the distance of each point from the line indicates the size of the discrepancy between the acquisition of neural and behavioral learning. The location of each point above or below the unity line indicates whether that neuron learned more or less quickly than did the behavior.

The FEF_{SEM} and the floccular complex differed in the extent to which the trial of neural learning acquisition matched that of the behavior. Neurons from the FEF_{SEM} (Figure 4A, open symbols) were fairly evenly distributed throughout the plot, at all distances from the unity line and about equally above or below the unity line. Most of the neurons from the floccular complex (filled symbols) were clustered near the unity line, with a minority displaced quite far from the line. In a histogram of the absolute difference between neural and behavioral learning acquisition (Figure 4B), the data from the FEF_{SEM} and the floccular complex had means that were not significantly different (19.3 trials, floccular complex; 25.5 trials, FEF_{SEM}; $p=0.08$; Mann-Whitney U test), but had significantly different distributions ($p=0.04$; Kolmogorov-Smirnov test). The floccular complex distribution was bimodal: 58% of the neurons acquired learning within 10 trials of the behavior, while another 21% differed from the behavior by between 50 to 60 trials. In contrast, the distribution from the FEF_{SEM} was flatter and broader: there were groups of neurons that differed from the behavior by anywhere between less than 10 (25% of the population) to more than 50 trials (12%), but no group was clearly predominant. Therefore, neurons in the floccular complex either acquired learning at roughly the same rate as the behavior, or differed considerably from the behavior, whereas learning acquisition in FEF_{SEM} neurons was much more distributed, with neurons differing from the behavior by anywhere between a small to a large number of trials.

To be sure that our results were not related to the choice of a 75% threshold for estimating the trial of learning acquisition, we repeated our findings using thresholds of 65% or 85%. We also obtained the same results with a “cross-correlation” method for estimating the leads and lags between the neural and behavioral learning curves, where we calculated the shift, in number of trials, needed to maximize the correlation between each pair of neural and behavioral learning curves.

To visualize how responses in the $\mathrm{FEF}_{\mathrm{SEM}}$ and the floccular complex evolve throughout the entire duration of the learning experiment, we created the representation shown in Figure 5A. After ordering all of the learning curves from each brain area by the trial at which the learning curve first reached 95% of its maximal value, we represented the learning curves on a color scale and plotted each learning curve along a horizontal line (Figure 5A). For both the floccular complex and the $\mathrm{FEF}_{\mathrm{SEM}}$, the colored summary of the learning curves reveals a diagonal red swath, indicating that each neuron shows a response that peaks for a specific trial during the learning experiment and then declines. Different neurons reached their peak response after a different number of learning trials. The red swatch of peaks is continuous for the $\mathrm{FEF}_{\mathrm{SEM}}$, but is slightly broken for the floccular complex, hinting at the existence of two distinct groups of neurons that respectively reach peak responses during early- and late-occurring learning trials. In contrast to the diversity in the trajectories of the neural learning curves, the behavioral learning curves in Figure 5B, which were in the order defined by their corresponding neural learning curves, had fairly stereotyped trajectories and maintained near-peak values throughout much of the learning experiment. As a result, the learned behavior was often maximal on trials where the expression of neural learning was weak. The opposite situation also occurred, although less frequently.

Inspection of Figure 5A suggests that neurons from the floccular complex whose responses peaked during the early learning trials exhibited a modest decrease in activity as learning progressed, whereas FEF_{SEM} neurons whose responses peaked early in learning tended to undergo a more drastic decrease in activity during later learning trials, with some neurons returning to baseline levels of activity. To quantify the differences in the maintenance of peak neural responses between the FEF_{SEM} and the floccular complex, we plotted each neuron's activity early in learning, defined as the mean value of the learning curve across the first 30 learning trials (learning trials #1 to #30), against its activity late in learning, defined as the mean value of the learning curve across the last 30 learning trials (learning trials #71 to #100) (Figure 5C).

In both brain areas, neurons weakly active early in learning tended to become highly active by the end of the learning experiment (Figure 5C). FEF_{SEM} neurons highly active early in learning subsequently showed decrements in their learned responses, causing the correlation between early learning activity and late learning activity across the FEF_{SEM} population to be significantly negative, at -0.44 (p=0.002). In contrast, neurons in the floccular complex whose activity peaked early in learning maintained an elevated level of activity up to the end of the learning experiment, reminiscent of the manner in which the behavior changed throughout learning. Therefore, the correlation for the floccular complex, 0.27, was not significantly different from zero (p=0.21). Removing an outlier data point located at (-0.05, -0.42), further decreased the correlation to 0.02. Finally, our findings were not dependent on the exact interval chosen for early and late learning; using the first/last 20 or 40 learning trials led to similar conclusions.

2.4.3 Time course of mean learned neural responses

We now move our focus to a comparison of how the mean learned response in the FEF_{SEM} and the floccular complex change as a function of time within the trial, and away from the analysis of learning curves that has comprised most of the paper. In agreement with earlier reports that different FEF_{SEM} neurons are most involved in pursuit at particular times during a pursuit movement (Schoppik et al., 2008; Li and Lisberger, 2011), we find similar features in the expression of learning in FEF_{SEM} neurons. Examples of the learned component of the mean firing rate as a function of time for two representative neurons (Figure 6A, B) show that the learned response of the neuron from the floccular complex (A) increased steadily over almost 200 ms up to the time of the instructive change in target direction, in parallel with the eye velocity of the learned behavior (B). In contrast, the firing rate of the example FEF_{SEM} neuron reached a peak before the time of the instructive change in target direction, even though the learned eye velocity continued to increase right up to the time of the instructive change in target direction.

The learned responses across the FEF_{SEM} population peaked at different times throughout the learned eye movement, while the peak times of the learned responses in the floccular complex were more uniform. Because neural responses tend to be noisy, we smoothed the raw firing rate traces with a 50 ms rectangular filter, and analyzed the smoothed results. To visualize the time courses of the collective mean learned neural and behavioral responses, we first normalized each learned response to have a maximal value of 1 and sorted them by the time at which the normalized neural response first reached

95% of its maximal value. We then plotted the ordered neural (Figure 6D) and behavioral (Figure 6E) responses as a series of colored lines, where pixel color encoded the magnitude of the normalized response at each time. In the floccular complex, the red swatch, which corresponds to the peaks of the learned neural responses, lies between 250 and 300 ms, indicating that the time course of the learned responses of Purkinje cells tended to exhibit a fairly stereotyped trajectory characterized by a monotonic increase up to the time of the instructive change in target direction, followed by a plateau. The FEF_{SEM} population shows a thin diagonal red swatch that extends from 100 to 300 ms, indicating that different FEF_{SEM} neurons were most active during distinct, brief movements in the learned eye movement. Collectively, the time of the peak responses in the FEF_{SEM} population spanned the duration of the learned eye movement. In contrast to the learned neural responses, the set of learned eye velocity traces failed to show a corresponding diagonal red swatch, indicating that the temporal diversity in the peaks of the FEF_{SEM} responses are unlikely to result from the heterogeneity in the peak times of the behavioral responses. On average, the difference between the latency to 95% of peak in learned neural responses versus learned behavioral responses averaged 35.8 ms for the floccular complex and 49.9 ms for the FEF_{SEM}.

Finally, we looked for a relationship between the peak time of the learned response in FEF_{SEM} neurons and the time during pre-learning pursuit when they are most active. We assessed the preferred time of each neuron during pre-learning pursuit in the direction ultimately chosen to be the learning direction, as the time when its mean firing rate over the first 320 milliseconds after the onset of target motion first reached 95% of its maximal value. As with the learned response, we analyzed the pre-learning response after it had been smoothed with a 50 ms rectangular filter. Plotting the time to 95% of the maximal response during pre-learning pursuit as a function of the time to 95% of the maximal learned response (Figure 6D) revealed that almost all neurons plotted on or below the unity line. Thus, the learned responses of FEF_{SEM} neurons tend to peak at the same time or later than their responses during pre-learning pursuit, at times that represent a compromise between the time contingencies of the learned behavior and the intrinsic preferred timing of each individual neuron.

2.5 Discussion

The motor cortex and the cerebellum act in concert to produce a broad range of movements; however, their respective roles during motor learning are not well understood. In this paper, we compared how activity in regions of the motor cortex and cerebellum associated with smooth pursuit, the FEF_{SEM} and the floccular complex, evolved across movement repetitions as the monkey gradually learned to produce an accurately-timed pursuit eye movement. Smooth pursuit is a useful system for studying motor learning because much is known about the function of specific areas throughout the neural circuit in generating the eye movement. Current models of the smooth pursuit neural circuit postulate the existence of two interacting pathways (Lisberger, 2010), one that uses visual motion signals to drive changes in eye velocity, and another that controls the extent to which incoming visual motion signals affect the motor command, also known as the gain of visual-motor transmission. The FEF_{SEM} is part of the gain control pathway (Tanaka and Lisberger, 2001, 2002), while the floccular complex is probably downstream from the site of convergence of the two pathways, and contains information related to the dynamics of the eye movement (Shidara et al., 1993; Krauzlis and Lisberger, 1994).

2.5.1 Functional mechanisms of pursuit learning

The findings in the present paper suggest that the mechanisms of pursuit learning are likely to involve changes in FEF_{SEM}, corresponding to a shift in the visual-motor gain, which may be coupled with separate changes in signal processing in the floccular complex. The details of the representation of learning in the FEF_{SEM} and the floccular complex are different, but in a manner consistent with the established functions of the two structures within the pursuit circuit. There was a looser link between behavioral learning and learning in individual neurons in the FEF_{SEM} versus the floccular complex. 58% of the neurons in the floccular complex acquired learning within 10 trials of the behavior, compared to 25% of the neurons in the FEF_{SEM}. Further, floccular complex neurons that acquired learning early on subsequently maintained elevated levels of activity throughout the remainder of the learning experiment, much like the learned behavior, while FEF_{SEM} neurons maintained their learned responses for only a brief number of trials once learning had been acquired. Finally, on a millisecond-by-millisecond basis, the trajectories of the mean learned responses of neurons from the floccular complex closely resembled those of the learned eye movement in that both increased monotonically starting from pursuit initiation and reached a maximum around the time of onset of the instructive change in target direction. In contrast, the learned responses of FEF_{SEM} neurons had more heterogeneous time courses, with different neurons maximally active at select moments throughout the duration of the learned eye movement. The output from the floccular complex behaved as if tightly linked to the movement itself, while FEF_{SEM} output appeared to reflect a compromise between the timing of the learned response and the intrinsic preferred time of the individual neuron.

Although learned responses in the FEF_{SEM} and the floccular complex differed somewhat at the level of individual neurons, the population representations of learning were surprisingly similar. Consistent with its role in encoding the motor command, the population average of the floccular complex evolved in step with changes in the learned eye velocity. Consistent with the prior suggestion that learned changes in pursuit eye movement might at least be partly driven by changes in the gain of visual-motor transmission (Chou and Lisberger, 2004), the population average in the FEF_{SEM} also evolved over learning trials along with the learned eye velocity. The population averages emerged from a considerably heterogeneous set of learning dynamics measured in individual neurons. In both brain areas, but more so in the FEF_{SEM} than in the floccular complex, only a fraction of neurons were highly active on any particular learning trial, and the identity of the maximally active neurons changed continuously throughout the duration of the learning experiment. We suggest that during different stages of learning, changes in the gain of visual-motor transmission and in the motor command are encoded by distinct subsets of neurons. The dynamics of the acquisition in individual neurons may provide information about the mechanisms of learning, while the population responses may tell us more about its final implementation.

2.5.2 Pursuit learning as a multi-rate process

Heterogeneity in the learning dynamics of neurons in both the floccular complex and the $\mathrm{FEF}_{\mathrm{SEM}}$ fits well with recent suggestions that motor learning arises from the interaction of multiple processes that adapt at different rates (Smith et al., 2006; Lee and Schweighofer, 2009; Yang and Lisberger, 2010). Unlike many earlier motor learning studies that focused on long-lasting neural changes occurring over days or even weeks (Medina et al., 2001; Kleim et al., 2004), we examined the evolution of neural activity throughout a single learning session, which consists of dozens of movements produced over the course of 10 to 20 minutes. Our finding of a broad diversity in the rate of learning acquisition across individual neurons after a few minutes of training provides direct evidence that even short-term motor learning is composed of a multitude of neural processes whose timescales of plasticity are incredibly varied and rich.

Work on smooth pursuit learning has provided some insight into the locations of different adaptive processes throughout the neural circuit. For example, a previous study using the same directional learning paradigm described here identified a form of rapid neural learning in the cerebellar cortex that occurs over a single trial (Medina and Lisberger, 2008). The findings in the present paper suggest two components of learning in the floccular complex: one in a group of cells that expressed neural learning after a relatively small number of learning trials and a second in a group of Purkinje cells that expressed learning only toward the end of a learning block. The two groups of Purkinje cells could be related to the theory (Miles and Lisberger, 1981; Krupa et al., 1993; Raymond et al., 1996; Medina et al., 2001; Nagao and Kitazawa, 2003; Kassardjian et al.,

2005) that that the motor memory initially forms in the cerebellar cortex, but is subsequently transferred to the deep cerebellar nuclei for long-term storage. The second group of neurons that did not become highly active until late in the learning process may play a special role in driving memory consolidation in the deep cerebellar nuclei, or may reflect a hitherto underappreciated form of long-term memory storage in the cerebellar cortex.

Our observation that the learned responses of different $\mathrm{FEF}_{\mathrm{SEM}}$ neurons reach their peak on different learning trials indicates that the $\mathrm{FEF}_{\mathrm{SEM}}$ is likely to also participate in multiple stages of motor learning. We found distinct groups of neurons that were recruited at the end of a learning block versus early in the learning block, indicating that the $\mathrm{FEF}_{\mathrm{SEM}}$ may not only play an important role in the consolidation of the memory trace, like what has been suggested for the primary motor cortex (Wise et al., 1998; Muellbacher et al., 2002; Paz et al., 2005; Richardson et al., 2006; Hadipour-Niktarash et al., 2007; Xu et al., 2009), but may also contribute to memory formation. However, because learned responses in the $\mathrm{FEF}_{\mathrm{SEM}}$ tended to have less sustained periods of elevated activity than responses in the floccular complex, the identity of the maximally active $\mathrm{FEF}_{\mathrm{SEM}}$ neurons evolved rapidly and continuously throughout the learning experiment. One interpretation could be that the $\mathrm{FEF}_{\mathrm{SEM}}$ contains a more detailed representation of the different stages of the learning process than the floccular complex.

Our data provide strong evidence that motor learning is a multi-site, multi-component behavioral phenomenon, but do not allow us to definitively pinpoint the neural substrates of the component adaptive processes. Indeed, because of the dense interconnectivity of the pursuit circuit, expressions of learning in the FEF_{SEM} and the floccular complex may reflect not local plasticity, but rather a response that is inherited from elsewhere in the pursuit circuit. Still, the heterogeneity in the dynamics of the expressions of learning in the two structures suggests that both rapid and slower forms of learning could arise independently in the FEF_{SEM} and in the floccular complex. We favor this scenario, because cellular and molecular studies are revealing an ever-increasing number of sites in both the cerebellum (Aizenman and Linden, 2000; Hansel and Linden, 2000; Zhang and Linden, 2006; Weeks et al., 2007; Pugh and Raman, 2008; Connor et al., 2009) and the cerebral cortex (for review, see Feldman, 2009) that are sensitive to multiple forms of physiological and structural plasticity with diverse temporal properties.

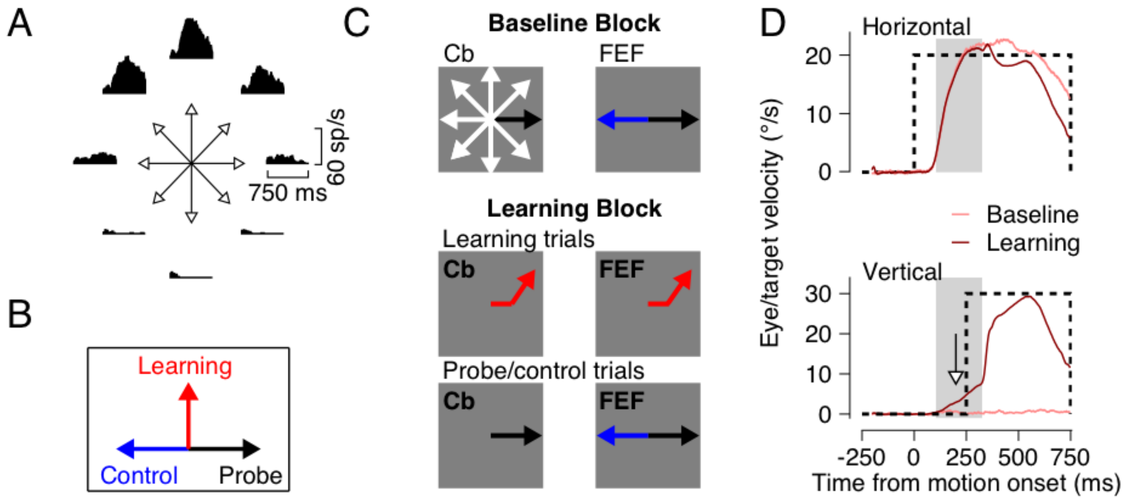

Figure 2.1: Behavioral learning paradigm.

(A) The direction tuning of an example neuron. (B) Top: The control (180°), probe (360°), and learning (90°) directions chosen for the neuron in A. (C) Trial configurations for the baseline block and the learning block, shown separately for the $\mathrm{FEF}_{\mathrm{SEM}}$ and floccular complex learning experiments. (D) Mean horizontal and vertical eye velocity traces from a single learning experiment. The red and pink traces show, respectively, the mean eye velocities from the learning trials and the probe trials in the baseline block, as a function of time from the onset of target motion. The gray shaded box indicates the analysis interval spanning 100 to 320 ms, and the black arrow denotes the learned behavioral response. The dashed black lines plot the target velocity from the learning trials.

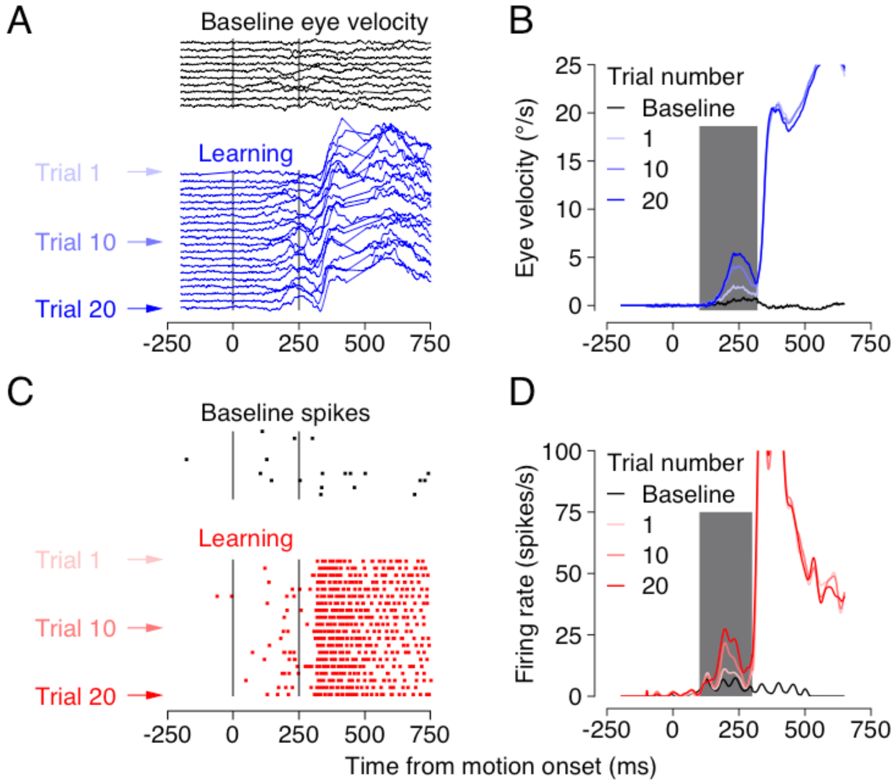

Figure 2.2: Trial-over-trial changes in the neural and behavioral responses within individual learning experiments.

The raw eye velocity traces (A) and spike trains (C) from the last 10 probe trials in the baseline block (black) and the first 20 learning trials from the learning block (blue: eye velocity, red: spike trains) are plotted as a function of time from the onset of target motion. The earliest trial is presented at the top. Note that the neural and behavioral data are from separate learning experiments. Smoothed eye velocity traces (B) and firing rate estimates (D) from the first, 10th, and 20th learning trials. The analysis interval (gray shaded box) spanned 100 to 300 ms for neural learning, and 100 to 320 ms for behavioral learning. The black traces plot the smoothed neural and behavioral data averaged across the last 10 probe trials from the baseline block.

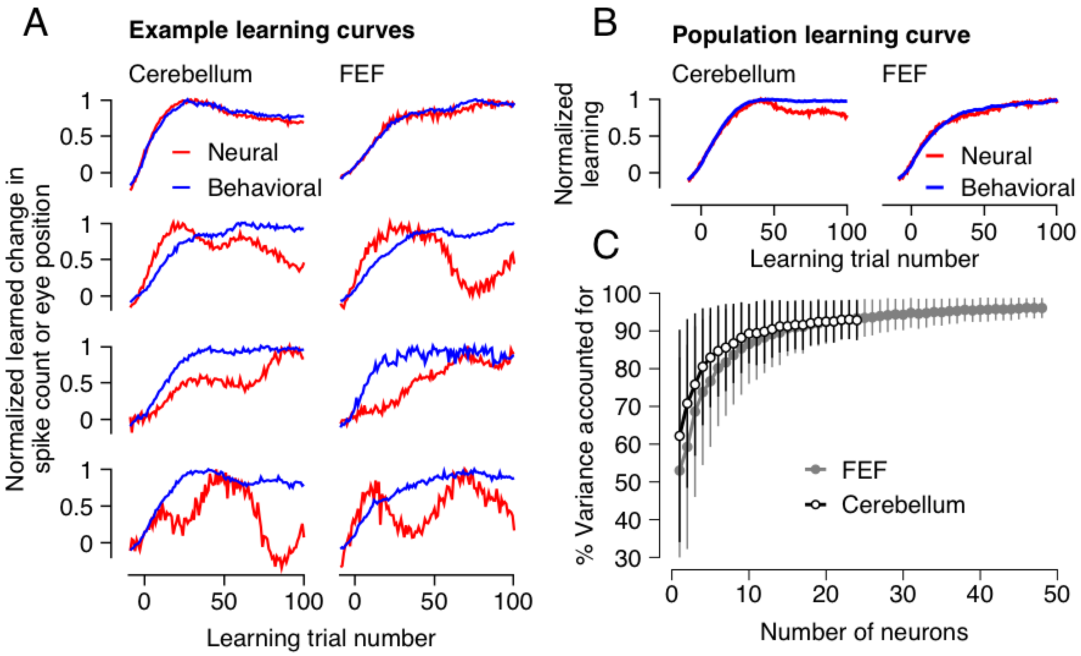

Figure 2.3: Comparison of behavioral learning curves with single-unit and population neural learning curves.

(A) Plots of the normalized learned change in spike count (red) or eye position (blue) as a function of the learning trial number. Each pair of neural and behavioral learning curves is from the same learning experiment, for a total of eight different learning experiments. (B) Normalized average of the full set of neural (red) and behavioral (blue) learning curves. (C) The percent variance in the average behavioral learning curve accounted for by the population neural learning curve is plotted as a function of the number of neurons in the population. Each symbol shows the mean percentage for a population with a given number of neurons; filled and open symbols represent data from the two brain areas. Error bars denote the 95% confidence intervals, calculated from the 1000 sample populations generated for each population size.

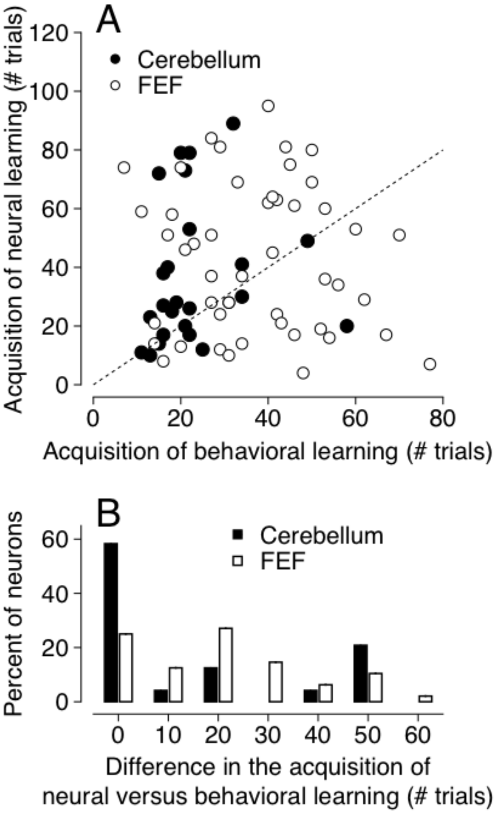

Figure 2.4: Acquisition of neural and behavioral learning.

(A) Plot of the trial of learning acquisition for the neural and behavioral responses. Each symbol represents data from a separate learning experiment. The dashed line has a slope of one. (B) Distribution of the difference, in number of trials, between the acquisition of neural and behavioral learning, for the FEF_{SEM} and the floccular complex.

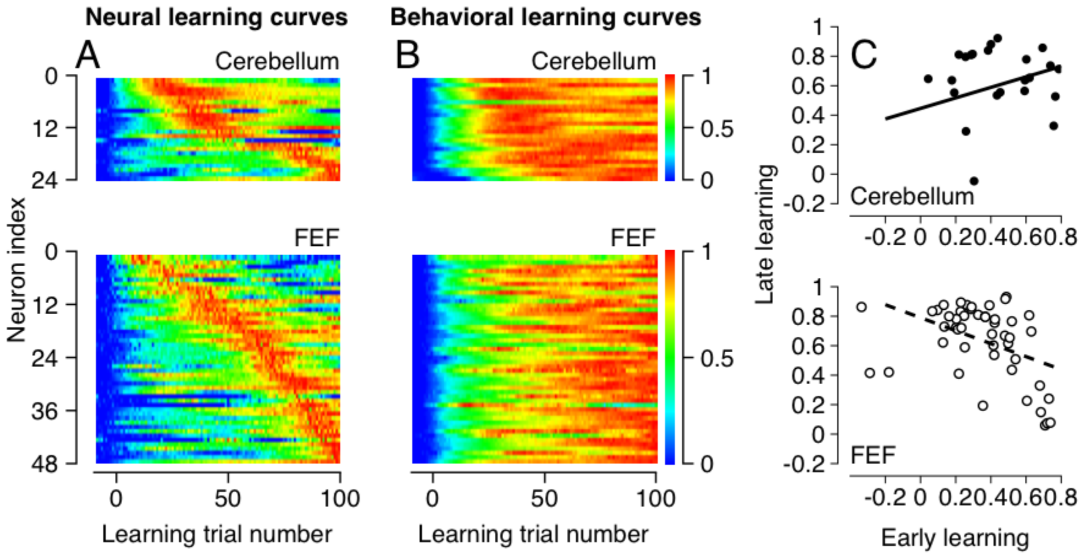

Figure 2.5: Neural and behavioral learning dynamics throughout the duration of the learning experiment.

(A) Summary of all 24 floccular complex (top) and 48 FEF_{SEM} learning curves (bottom) in our sample. Each line uses color to plot the value of a single learning curve as a function of learning trial number. Neurons are ordered from top to bottom by the trial at which their learning curve first reached 95% of maximum. (B) Behavioral learning curves are plotted in the order in which the neural learning curves from the same learning experiment appeared in A. (C) A plot of the mean value of the learning curve across the first 30 (early) versus the last 30 (late) learning trials, for the full set of neurons in floccular complex (top) and the FEF_{SEM} (bottom). Each symbol represents data from a single neuron, and the line in each graph is the linear regression fit to the population data.

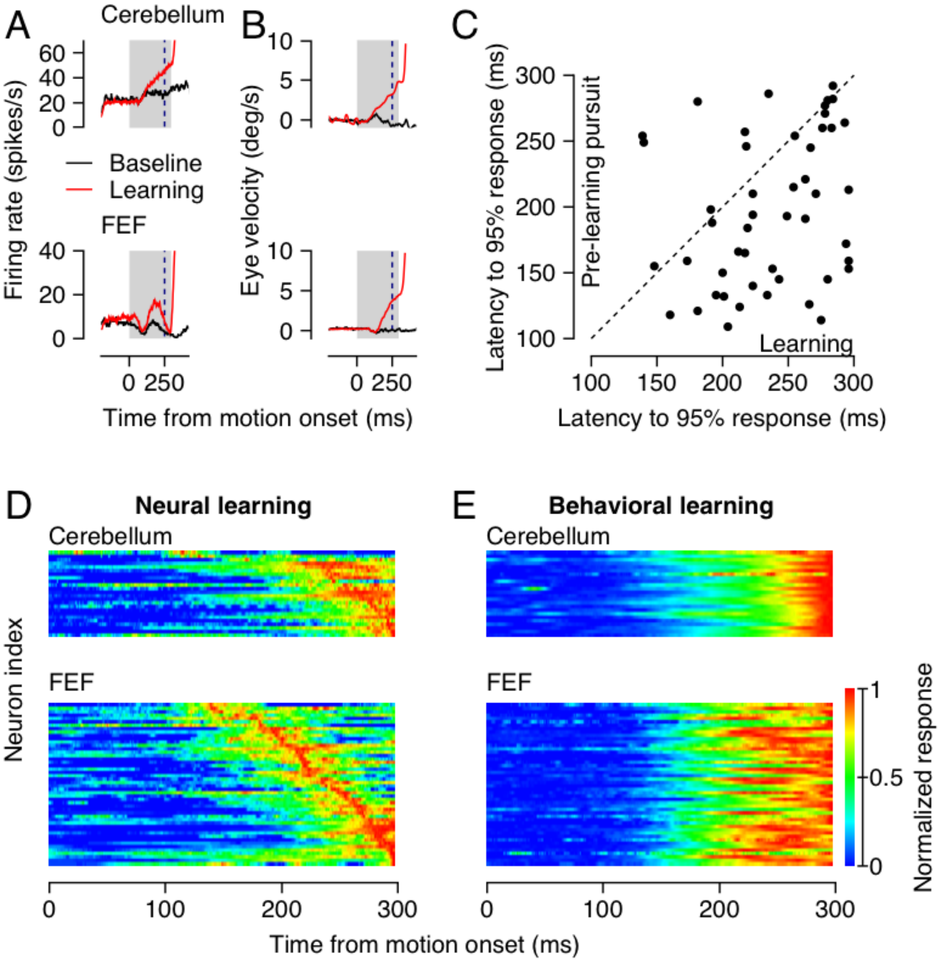
A
Cerebellum
60
40
20
0
Firing rate (spikes/s)
Baseline
Learning
FEF
40
20
0
0 250
B
10
5
0
Eye velocity (deg/s)
10
5
0
0 250
Time from motion onset (ms)
C
300
250
200
150
100
Latency to 95% response (ms)
Pre-learning pursuit
Learning
100 150 200 250 300
Latency to 95% response (ms)
D
Neural learning
Cerebellum
FEF
Neuron index
E
Behavioral learning
Cerebellum
FEF
1
0.5
0
Normalized response
0 100 200 300
0 100 200 300
Time from motion onset (ms)

Figure 2.6: Analysis of the time course of the mean learned neural and behavioral responses.

(A) Mean firing rates of a representative floccular complex (top) and FEF_{SEM} (bottom) neuron, plotted as a function of time from the onset of target motion. (B) The mean eye velocities traces from the learning experiments shown in A. Black and red traces represent, respectively, data from the probe trials in the baseline block and from the learning trials. The grey shaded boxes in A and B, which span 1 to 296 ms, delineate the interval of the learned response plotted in C and D. (C) For each of the 48 FEF_{SEM} neurons, we plot the time at which its pre-learning response first reaches 95% of maximum, against the time at which its learned response first reaches 95% of maximum. Each symbol shows data from a separate neuron, and the dashed line has a slope of one. (D) Color maps of the normalized mean learned responses for all 24 floccular complex (top) and 48 FEF_{SEM} (bottom) neurons. Each line uses color to plot the magnitude of the normalized learned response of a single neuron as a function of time from the onset of target motion. Responses are ordered from top to bottom according to their latency to 95% of maximum. (E) The normalized mean learned behavioral responses, sorted by the order in which the neural responses from the same learning experiment appeared in D.

General Discussion

The element of time shapes all aspects of motor control. The brain must be capable of processing time within a single movement, i.e., when to strike the ball during a tennis serve, as well as improving the serve with practice. In this thesis, I used a simple ocular tracking behavior, smooth pursuit, to probe the neural basis of the dynamics of motor learning, both within a single movement and across repetitions of the movement. I recorded the responses of single neurons in the motor cortex of the pursuit circuit, the FEF_{SEM}, as the monkey learned to produce a temporally precise smooth eye movement, and compared the results from the FEF_{SEM} with previously published data from the floccular complex of the cerebellum, another site that has been implicated in pursuit learning (Medina et al., 2008).

By relating the magnitude of learning expressed by the neuron with its innate sensitivity to elapsed time within a movement, I demonstrated that the FEF_{SEM} might be an important source of within-movement timing signals during learning. A comparison of how the learned responses in the FEF_{SEM} and the floccular complex evolved across movements as the animal acquired and practiced the learned eye movement suggested that the two brain areas may participate in multiple aspects of the learning process, and that their roles are likely to be at least partially distinct.

This thesis illustrates that characterizing the pattern of learned responses across the population can provide insight into the function of a given brain area during learning. FEF_{SEM} neurons that preferred the timing of the instructive stimulus expressed greater amounts of learning, indicating that the pursuit circuit makes use of the temporal information in the FEF_{SEM} during motor learning. Similarly, the across-movement response dynamics in the FEF_{SEM} and the floccular complex led to the conclusion that the two areas may be involved in different facets of the learning process, and provided some insight into what those facets might be. However, one major drawback of inferring brain function based on the form of the neural responses is the inability to establish causality. In the following paragraphs, I have proposed a series of experiments aimed towards bridging this gap.

In light of the results presented in Chapter 1, how might one demonstrate that the within-movement temporal map in the FEF_{SEM} is *necessary* for producing an appropriately-timed learned eye movement? Throughout the cerebral cortex, neural selectivity to specific stimulus features appears to arise partly as a result of GABAergic inhibition (Li et al., 2008; Allito and Dan, 2010; Wu et al., 2008). Thus, it might be possible to make FEF_{SEM} neurons less selective for distinct times during pursuit by blocking GABA transmission via muscimol or bicuculline, and then asking whether the learned eye movement loses its temporal precision. Since proper execution of smooth pursuit requires an intact FEF_{SEM} (Keating, 1991; Macavoy et al., 1991), it would be necessary to eliminate a general motor deficit as the cause of any changes in the learned behavior. Similarly, one might manipulate the temporal map of the FEF_{SEM} in other, less invasive ways, and relate changes in the precision of the neural representation of time to corresponding shifts in the temporal specificity of the learned eye movement. For example, long-term exposure to pursuit trials where target motion lasts not for 750 ms, but for 400 ms or 1600 ms, may cause FEF_{SEM} neurons to refine or broaden their temporal selectivity, which may in turn lead to learned eye movements that are more or less temporally precise.

The results presented in Chapters 1 and 2 provide some clues about the involvement of the FEF_{SEM} and the floccular complex in pursuit learning, but fail to specify whether plasticity in either structure is *necessary* for any aspect of pursuit learning. A classical approach for establishing necessity is to lesion the brain area or block excitatory neurotransmission via application of a variety of drugs. Unfortunately, because the FEF_{SEM} (Keating, 1991; Macavoy et al., 1991) and the floccular complex (Rambold et al., 2002), are necessary for normal smooth pursuit performance, it will be difficult to distinguish whether learning deficits are related specifically to a lack of plasticity in the FEF_{SEM} or the floccular complex, or are secondary to general problems in motor execution. However, it might be possible to use a variety of molecular techniques to selectively block the induction of plasticity, but allow for signal transmission. CamKII is a calcium binding protein that is not required for basic neuronal function, but is critical for activity-dependent synaptic plasticity (Silva et al., 1992a); blocking CamKII activity impairs learning (Silva et al., 1992b). To selectively inactivate CamKII in the FEF_{SEM} or the floccular complex, we could use a virus vector to deliver either CamKII siRNA, or inject a membrane permeable CamKII inhibitor, such as KN-93, and monitor the effects on various properties of pursuit learning, such as the size of the learned eye movement, the rate of learning acquisition, and the stability of the motor memory, to name a few. We can also use a similar approach to test other candidate molecules with available inhibitors, such as protein kinase M zeta, which appears to be selectively involved in the maintenance of long-term memories (Pastalkova et al., 2006; Shema et al., 2007), including sensorimotor memories (von Kraus et al., 2010).

An alternative to directly blocking plasticity in the $\mathrm{FEF}_{\mathrm{SEM}}$ or the floccular complex is to corrupt processing of the visual error caused by the instructive change in target direction. One could use electrical or optogenetic methods to briefly inhibit the brain area around the time at which the visual error signal is expected to arrive, which is approximately 70 ms after the instruction time for the $\mathrm{FEF}_{\mathrm{SEM}}$ (Li and Lisberger, 2011) and 75 to 175 ms for the floccular complex (Medina and Lisberger, 2008). Finally, it may be possible to selectively prevent plasticity in the flocculus by perturbing the inferior olive, which is a direct source of the visual error signal for the floccular complex, but not for the $\mathrm{FEF}_{\mathrm{SEM}}$ (Simpson, 1984; Langer et al., 1985; Voogd and Barmack, 2006).

Although data presented in this thesis implicated the $\mathrm{FEF}_{\mathrm{SEM}}$ in specifying the timing of the learned eye movement, there is evidence suggesting that the cerebellar cortex also plays an important role in motor timing (Perrett et al., 1993). Therefore, the manipulations proposed above would additionally be useful for disentangling the respective contributions of the two brain areas to the within-movement temporal specificity of the learned behavior.

In each pursuit learning experiment, the first few exposures to the instructive stimulus elicit large learned changes in the eye movement, but subsequent exposures to the same stimulus produce successively more modest behavioral improvements, consistent with what is typically observed during motor learning. However, a growing body of evidence from other motor learning tasks indicates that training affects more than just the dynamics of the movement: in a task where subjects were required to perform a rapid sequence of finger movements, training on one hand initially improved the performance of the contralateral hand for the same movement sequence. However, additional training on the original hand resulted in improvements that were restricted to the trained hand (Korman et al., 2003). Extended training has also been shown to make the memory trace more robust (Yin and Kitazawa, 2001; Joiner and Smith, 2008). In one instance, overtraining on a visuomotor rotation task partially blocked the retrograde interference induced upon subsequent learning of a counter-rotation (Krakauer et al., 2005). Therefore, the number of times the system experiences the instructive stimulus has important implications for not only the amount of behavioral learning expressed by the animal, but also the specificity and stability of the learned behavior. An interesting avenue of future research would be to determine 1) whether the robustness and the directional and temporal specificity of the smooth pursuit memory trace change as a function of training, 2) the properties and time scales of these changes, and 3) the characteristics of the responsible neural mechanisms and their locations within the pursuit circuit.

In conclusion, I have only explored a small corner of the rich space of motor learning. Motor learning does not saturate with a single training session, but can further develop over hours, days, or even years, and is likely to engage a dynamic network of brain areas. Careful behavioral studies, coupled with recordings from multiple locations within the smooth pursuit circuit, will set the stage for a more complete understanding of how the intricate interplay of neural signals gives rise to all facets of motor learning.

References

Aizenman, C.D., and Linden, D.J. (2000). Rapid, synaptically driven increases in the intrinsic excitability of cerebellar deep nuclear neurons. Nat Neurosci. *3*, 109-11.

Alitto, H.J., and Dan, Y. (2010). Function of inhibition in visual cortical processing. Curr Opin Neurobiol. *20*, 340-6.

Arce, F., Novick, I., Mandelblat-Cerf, Y., Israel, Z., Ghez, C., and Vaadia, E. (2010). Combined adaptiveness of specific motor cortical ensembles underlies learning. J Neurosci. *30*, 5415-25.

Bi, G.Q., and Poo, M.M. (1998). Synaptic modifications in cultured hippocampal neurons: dependence on spike timing, synaptic strength, and postsynaptic cell type. J Neurosci. *18*, 10464-72.

Brown, E.M., Nguyen, D.P., Frank, L.M., Wilson, M.A., and Solo, V. (2001). An analysis of neural receptive field plasticity by point process adaptive filtering. Proc Natl Acad Sci U S A. *98*, 12261-6.

Buonomano, D.V. (2005). A learning rule for the emergence of stable dynamics and timing in recurrent networks. J Neurophysiol. *94*, 2275-83.

Buonomano, D.V., and Karmarkar, U.R. (2002). How do we tell time? Neuroscientist. *8*, 42-51.

Buonomano, D.V., and Mauk, M.D. (1994). Neural network model of the cerebellum: temporal discrimination and the timing of motor responses. Neural Comput. *6*, 38–55.

Cajou, S.R., van der Kamp, J., and Savelsbergh, G.J. (2004). Catching optical information for the regulation of timing. Exp Brain Res. *155*, 427-38.

Carey, M.R., Medina, J.F., and Lisberger, S.G. (2005). Instructive signals for motor learning from visual cortical area MT. Nat Neurosci. *8*, 813-9.

Chiba, A., Oshio, K., and Inase, M. (2008). Striatal neurons encoded temporal information in duration discrimination task. Exp Brain Res. *186*, 671-6.

Chou, I.H., and Lisberger, S.G. (2004). The role of the frontal pursuit area in learning in smooth pursuit eye movements. J Neurosci. *24*, 4124-33.

Chukoskie, L., and Movshon, J.A. (2009). Modulation of visual signals in macaque MT and MST neurons during pursuit eye movement. J Neurophysiol. *102*, 3225-33.

Churchland, M.M., and Shenoy, K.V. (2007). Temporal complexity and heterogeneity of single-neuron activity in premotor and motor cortex. J Neurophysiol. *97*, 4235-57.

Connor, S., Bloomfield, J., LeBoutillier, J.C., Thompson, R.F., Petit, T.L., and Weeks, A.C. (2009). Eyeblink conditioning leads to fewer synapses in the rabbit cerebellar cortex. Behav Neurosci. *123*, 856-62.

Cui, D.M., Yan, Y.J., and Lynch, J.C. (2003). Pursuit subregion of the frontal eye field projects to the caudate nucleus in monkeys. J Neurophysiol. *89*, 2678-84.

Doyon, J., Bellec, P., Amsel, R., Penhune, V., Monchi, O., Carrier, J., Lehéricy, S., and Benali, H. (2009). Contributions of the basal ganglia and functionally related brain structures to motor learning. Behav Brain Res. *199*, 61-75.

Ethier, V., Zee, D.S., and Shadmehr, R. (2008). Spontaneous recovery of motor memory during saccade adaptation. J Neurophysiol. *99*, 2577-83.

Evarts, E. (1968). Relation of pyramidal tract activity to force exerted during voluntary movement. J. Neurophysiol. *31*, 14-27.

Feldman, D.E. (2009). Synaptic mechanisms for plasticity in neocortex. Annu Rev Neurosci. *32*, 33-55.

Frank, L.M., Eden, U.T., Solo, V., Wilson, M.A., and Brown, E.N. (2002). Contrasting patterns of receptive field plasticity in the hippocampus and the entorhinal cortex: an adaptive filtering approach. J Neurosci. *22*, 3817-30.

Georgopoulos, A.P., Kalaska, J.F., Caminiti, R., and Massey, J.T. (1982). On the relations between the direction of two-dimensional arm movements and cell discharge in primate motor cortex. J Neurosci. *2*,1527-37.

Gottlieb, J.P., MacAvoy, M.G., and Bruce, C.J. (1994). Neural responses related to smooth-pursuit eye movements and their correspondence with electrically elicited smooth eye movements in the primate frontal eye field. J Neurophysiol. *72*, 1634-53.

Hadipour-Niktarash, A., Lee, C.K., Desmond, J.E., and Shadmehr, R. (2007). Impairment of retention but not acquisition of a visuomotor skill through time-dependent disruption of primary motor cortex. J Neurosci. *49*, 13413-9.

Hansel, C., and Linden, D.J. (2000). Long-term depression of the cerebellar climbing fiber--Purkinje neuron synapse. Neuron. *26*, 473-82.

Hatsopoulos, N.G., Xu, Q., and Amit, Y. (2007). Encoding of movement fragments in the motor cortex. J Neurosci. *27*, 5105-14.

de Hemptinne, C., Nozaradan, S., Duvivier, Q., Lefèvre, P., and Missal, M. (2007). How do primates anticipate uncertain future events? J Neurosci. *27*, 4334-41.

Ivry, R.B. (1996). The representation of temporal information in perception and motor control. Curr Opin Neurobiol. *6*, 851-7.

Jin, D.Z., Fujii, N., and Graybiel, A.M. (2009). Neural representation of time in cortico-basal ganglia circuits. Proc Natl Acad Sci U S A. *106*, 19156-61.

Joiner, W.M., and Smith, M.A. (2008). Long-term retention explained by a model of short-term learning in the adaptive control of reaching. J Neurophysiol. *100*, 2948-55.

Kahlon, M., and Lisberger, S.G. (1996). Coordinate system for learning in the smooth pursuit eye movements of monkeys. J Neurosci. *16*, 7270-83.

Kahlon, M., and Lisberger, S.G. (2000). Changes in the responses of Purkinje cells in the floccular complex of monkeys after motor learning in smooth pursuit eye movements. J Neurophysiol. *84*, 2945-60.

Kassardjian, C.D., Tan, Y.F., Chung, J.Y., Heskin, R., Peterson, M.J., and Broussard, D.M. (2005). The site of a motor memory shifts with consolidation. J Neurosci. *25*, 7979-85.

Keating , E.G. (1991). Frontal eye field lesions impair predictive and visually-guided pursuit eye movements. Exp Brain Res. *86*, 311-23.

Kleim, J.A., Hogg, T.M., VandenBerg, P.M., Cooper, N.R., Bruneau, R., and Remple, M. (2004). Cortical synaptogenesis and motor map reorganization occur during late, but not early, phase of motor skill learning. J Neurosci. *24*, 628-33.

Korman, M., Raz, N., Flash, T., and Karni, A. (2003). Multiple shifts in the representation of a motor sequence during the acquisition of skilled performance. Proc Natl Acad Sci U S A. *100*, 12492-7.

Krakauer, J.W., Ghez, C., and Ghilardi, M.F. (2005). Adaptation to visuomotor transformations: consolidation, interference, and forgetting. J Neurosci. *25*, 473-8.

Krauzlis, R.J. (2004). Recasting the smooth pursuit eye movement system. J Neurophysiol. *91*, 591-603.

Krauzlis, R.J., and Lisberger, S.G. (1994). Simple spike responses of gaze velocity Purkinje cells in the floccular lobe of the monkey during the onset and offset of pursuit eye movements. J Neurophysiol. *72*, 2045-50.

Krauzlis, R.J., and Lisberger, S.G. (1996). Directional organization of eye movement and visual signals in the floccular lobe of the monkey cerebellum. Exp Brain Res. *109*, 289-302.

Krupa, D.J., Thompson, J.K., and Thompson, R.F. (1993). Localization of a memory trace in the mammalian brain. Science. *260*, 989-91.

Langer, T., Fuchs, A.F., Scudder, C.A., and Chubb, M.C. (1985). Afferents to the flocculus of the cerebellum in the rhesus macaque as revealed by retrograde transport of horseradish peroxidase. J Comp Neurol. *235*, 1-25.

Lee, J.Y., and Schweighofer, N. (2009). Dual adaptation supports a parallel architecture of motor memory. J Neurosci. *29*, 10396-404.

Leichnetz, G.R. (1989). Inferior frontal eye field projections to the pursuit-related dorsolateral pontine nucleus and middle temporal area (MT) in the monkey. Vis Neurosci. *3*,171-80.

Leon, M.I., and Shadlen, M.N. (2003). Representation of time by neurons in the posterior parietal cortex of the macaque. Neuron. *38*, 317-27.

Lewis, P.A., and Miall, R.C. (2003). Brain activation patterns during measurement of sub- and supra-second intervals. Neuropsychologia. *41*,1583-92.

Li, G., Yang, Y., Liang, Z., Xia, J., and Zhou, Y. (2008). GABA-mediated inhibition correlates with orientation selectivity in primary visual cortex of cat. Neuroscience. *155*, 914-22.

Li, J.X., and Lisberger, S.G. (2011). Learned timing of motor behavior in the smooth eye movement region of the frontal eye fields. Neuron. *69*, 159-69.

Lisberger, S.G. (2010). Visual guidance of smooth-pursuit eye movements: sensation, action, and what happens in between. Neuron. *66*, 477-91.

Lynch, J.C. (1987). Frontal eye field lesions in monkeys disrupt visual pursuit. Exp Brain Res. *68*, 437-41.

MacAvoy, M.G., Gottlieb, J.P., and Bruce, C.J. (1991). Smooth-pursuit eye movement representation in the primate frontal eye field. Cereb Cortex. *1*, 95-102.

Malenka, R.C., and Bear, M.F. (2004). LTP and LTD: An Embarrassment of Riches. Neuron. *44*, 5-21.

Mauk, M.D., and Buonomano, D.V. (2004). The neural basis of temporal processing. Annu Rev Neurosci. *27*, 307-40.

Mauk, M.D., and Ruiz, B.P. (1992). Learning-dependent timing of Pavlovian eyelid responses: differential conditioning using multiple interstimulus intervals. Behav Neurosci. *106*, 666-81.

Medina, J.F., Garcia, K.S., and Mauk, M.D. (2001). A mechanism for savings in the cerebellum. J Neurosci. *21*, 4081-9.

Medina, J.F., Carey, M.R., and Lisberger, S.G. (2005). The representation of time for motor learning. Neuron. *45*, 157-67.

Medina, J.F., and Lisberger, S.G. (2008). Links from complex spikes to local plasticity and motor learning in the cerebellum of awake-behaving monkeys. Nat Neurosci. *11*, 1185-92.

Medina, J.F., and Lisberger, S.G. (2009). Encoding and decoding of learned smooth-pursuit eye movements in the floccular complex of the monkey cerebellum. J Neurosci. *102*, 2039-54.

Muellbacher, W., Ziemann, U., Wissel, J., Dang, N., Kofler, M., Facchini, S., Boroojerdi, B., Poewe, W., and Hallett, M. (2002). Early consolidation in human primary motor cortex. Nature. 415, *640*-4.

Miles, F.A., and Lisberger, S.G. (1981). Plasticity in the vestibulo-ocular reflex: a new hypothesis. Annu Rev Neurosci. *4*, 273-99.

Moran, D.W. and Schwartz, A.B. (1999). Motor cortical representation of speed and direction during reaching. J. Neurophysiol. *82*, 2676-2692.

Nagao, S., and Kitazawa, H. (2003). Effects of reversible shutdown of the monkey flocculus on the retention of adaptation of the horizontal vestibulo-ocular reflex. Neuroscience. *118*, 563-70.

Newsome, W.T., Wurtz, R.H., and Komatsu, H. (1988). Relation of cortical areas MT and MST to pursuit eye movements. II. Differentiation of retinal from extraretinal inputs. J Neurophysiol. *60*, 604-20.

Ono, S., Das, V.E., Economides, J.R., and Mustari, M.J. (2005). Modeling of smooth pursuit-related neuronal responses in the DLPN and NRTP of the rhesus macaque. J Neurophysiol. *93*,108-16.

Ono, S., and Mustari, M.J. (2006). Extraretinal signals in MSTd neurons related to volitional smooth pursuit. J Neurophysiol. *96*, 2819-25.

Onoe, H., Komori, M., Onoe, K., Takechi, H., Tsukada, H., and Watanabe, Y. (2001). Cortical networks recruited for time perception: a monkey positron emission tomography (PET) study. Neuroimage. *13*, 37-45.

Oshio, K., Chiba, A., and Inase, M. (2006). Delay period activity of monkey prefrontal neurones during duration-discrimination task. Eur J Neurosci. *23*, 2779-90.

Pastalkova, E., Serrano, P., Pinkhasova, D., Wallace, E., Fenton, A.A., and Sacktor, T.C. (2006). Storage of spatial information by the maintenance mechanism of LTP. Science. *313*, 1141-4.

Paz, R., Boraud, T., Natan, C., Bergman, H., and Vaadia, E. (2003). Preparatory activity in motor cortex reflects learning of local visuomotor skills. Nat Neurosci. *6*, 882-90.

Paz, R., Natan, C., Boraud, T., Bergman, H., and Vaadia, E. (2005). Emerging patterns of neuronal responses in supplementary and primary motor areas during sensorimotor adaptation. J Neurosci. *25*, 10941-51.

Perrett, S.P., Ruiz, B.P., and Mauk, M.D. (1993). Cerebellar cortex lesions disrupt learning-dependent timing of conditioned eyelid responses. J Neurosci. *13*, 1708-18.

Pugh, J.R., and Raman, I.M. (2008). Mechanisms of potentiation of mossy fiber EPSCs in the cerebellar nuclei by coincident synaptic excitation and inhibition. J Neurosci. *28*, 10549-60.

Ramachandran, R., and Lisberger, S.G. (2005). Normal performance and expression of learning in the vestibulo-ocular reflex (VOR) at high frequencies. J Neurophysiol. *93*, 2028-38.

Rambold, H., Churchland, A., Selig, Y., Jasmin, L., and Lisberger, S.G. (2002). Partial ablations of the flocculus and ventral paraflocculus in monkeys cause linked deficits in smooth pursuit eye movements and adaptive modification of the VOR. J Neurophysiol. *87*, 912-24.

Rashbass, C. (1961). The relationship between saccadic and smooth tracking eye movements. J Physiol. *159*, 326-38.

Raymond, J.L., Lisberger, S.G., and Mauk, M.D. (1996). The cerebellum: a neuronal learning machine? Science. *272*, 1126-31.

Rao, S.M., Mayer, A.R., and Harrington D.L. (2001). The evolution of brain activation during temporal processing. Nat Neurosci. *4*, 317-23.

Recanzone, G., Schreiner, C., and Merzenich, M. (1993). Plasticity in the frequency representation of primary auditory cortex following discrimination training in adult owl monkeys. J Neurosci. *13*, 87-103.

Regan, D., and Gray, R. (2000). Visually guided collision avoidance and collision achievement. Trends Cogn. Sci. *4*, 99–107.

Richardson, A.G., Overduin, S.A., Valero-Cabre, A., Padoa-Schioppa, C., Pascual-Leone, A., Bizzi, E., and Press, D.Z. (2006). Disruption of primary motor cortex before learning impairs memory of movement dynamics. J Neurosci. *26*, 12466-70.

Sakurai, Y., Takahashi, S., and Inoue, M. (2004). Stimulus duration in working memory is represented by neuronal activity in the monkey prefrontal cortex. Eur J Neurosci. *20*, 1069-80.

Schoppik, D., Nagel, K.I., and Lisberger, S.G. (2008). Cortical mechanisms of smooth eye movements revealed by dynamic covariations of neural and behavioral responses. Neuron. *58*, 248-60.

Schoups, A., Vogels, R., Qian, N., and Orban, G. (2001). Practising orientation identification improves orientation coding in V1 neurons. Nature. *412*, 549-53.

Sharpe, J.A. (2008). Neurophysiology and neuroanatomy of smooth pursuit: lesion studies. Brain Cogn. *68*, 241-54.

Shema, R., Sacktor, T.C., and Dudai, Y. (2007). Rapid erasure of long-term memory associations in the cortex by an inhibitor of PKM zeta. *317*, 951-3.

Sherk, H., and Fowler, G.A. (2001). Neural analysis of visual information during locomotion. Prog Brain Res. *134,* 247-64.

Shidara, M., Kawano, K., Gomi, H., and Kawato, M. (1993). Inverse-dynamics model eye movement control by Purkinje cells in the cerebellum. Nature. *365*, 50-2.

Shih, L.Y., Kuo, W.J., Yeh, T.C., Tzeng, O.J., and Hsieh, J.C. (2009). Common neural mechanisms for explicit timing in the sub-second range. Neuroreport. *20*, 897-901.

Simpson, J. I. (1984). The accessory optic system. Annu Rev Neurosci. *7*, 13-41.

Silva, A.J., Paylor, R., Wehner, J.M., and Tonegawa, S. (1992a). Impaired spatial learning in alpha-calcium-calmodulin kinase II mutant mice. Science. *257*, 206-11.

Silva, A.J., Stevens, C.F., Tonegawa, S., Wang, Y. (1992b). Deficient hippocampal long-term potentiation in alpha-calcium-calmodulin kinase II mutant mice. Science. *257*, 201-6.

Smith, A., Taylor, E., Lidzba, K., and Rubia, K. (2003). A right hemispheric frontocerebellar network for time discrimination of several hundreds of milliseconds. Neuroimage. *20*, 344-50.

Smith, M.A., Ghazizadeh, A., and Shadmehr, R. (2006). Interacting adaptive processes with different timescales underlie short-term motor learning. PLoS Biol. *4*, e179.

Squatrito, S, and Maioli, M.G. (1997). Encoding of smooth pursuit direction and eye position by neurons of area MSTd of macaque monkey. J Neurosci. *17*, 3847-60.

Stanton, G.B., Friedman, H.R., Dias, E.C., and Bruce, C.J. (2005). Cortical afferents to the smooth-pursuit region of the macaque monkey's frontal eye field. Exp Brain Res. *165*, 179-92.

Stone, L.S., and Lisberger, S.G. (1990). Visual responses of Purkinje cells in the cerebellar flocculus during smooth-pursuit eye movements in monkeys. I. Simple spikes. J Neurophysiol. *63*, 1241-61.

Tanaka, M., and Lisberger, S.G. (2001). Regulation of the gain of visually guided smooth-pursuit eye movements by frontal cortex. Nature. *409*, 191-4.

Tanaka. M., and Lisberger, S.G. (2002). Enhancement of multiple components of pursuit eye movement by microstimulation in the arcuate frontal pursuit area in monkeys. J Neurophysiol. *87*, 802-18.

Von Kraus, L.M., Sacktor, T.C., and Francis, J.T. (2010). Erasing sensorimotor memories via PKM zeta inhibition. PLoS One. *5*, e11125.

Voogd, J., and Barmack, N.H. (2006). Oculomotor cerebellum. Prog Brain Res. *151*, 231-68.

Weeks, A.C., Connor, S., Hinchcliff, R., LeBoutillier, J.C., Thompson, R.F., and Petit, T.L. (2007). Eye-blink conditioning is associated with changes in synaptic ultrastructure in the rabbit interpositus nuclei. Learn Mem. *14*, 385-9.

Westheimer, G., and Blair, S.M. (1973). Oculomotor defects in cerebellectomized monkeys. Invest Ophthalmol. *12*, 618-21.

Wirth, S., Yanike, M., Frank, L.M., Smith, A.C., Brown, E.N., and Suzuki, W.A. (2003). Single neurons in the monkey hippocampus and learning of new associations. Science. *300*, 1578-81.

Wise, S.P., Moody, S.L., Blomstrom, K.J., and Mitz, A.R. (1998). Changes in motor cortical activity during visuomotor adaptation. Exp Brain Res. *121*, 285-99.

Wu, G.K., Arbuckle, R., Liu, B.H., Tao, H.W., and Zhang, L.I. (2008). Lateral sharpening of cortical frequency tuning by approximately balanced inhibition. Neuron. *58*, 132-43.

Xu, T., Yu, X., Perlik, A. J., Tobin, W. F., Zweig, J. A., Tennant, K., Jones, T., and Zuo, Y. (2009). Rapid formation and selective stabilization of synapses for enduring motor memories. Nature. *462*, 915-9.

Yang, Y., and Lisberger, S.G. (2010). Learning on multiple time scales in smooth pursuit eye movements. J Neurophysiol. *104*, 2850-62.

Yin, P.B., and Kitazawa, S. (2001). Long-lasting aftereffects of prism adaptation in the monkey. Exp Brain Res. *141*, 250-3.

Yang, T., and Maunsell, J.H. (2004). The effect of perceptual learning on neuronal responses in monkey visual area V4. J Neurosci. *24*, 1617-26.

Zhang, W., and Linden, D.J. (2006). Long-term depression at the mossy fiber-deep cerebellar nucleus synapse. J Neurosci. *26*, 6935-44.

Publishing Agreement

It is the policy of the University to encourage the distribution of all theses, dissertations, and manuscripts. Copies of all UCSF theses, dissertations, and manuscripts will be routed to the library via the Graduate Division. The library will make all theses, dissertations, and manuscripts accessible to the public and will preserve these to the best of their abilities, in perpetuity.

Please sign the following statement: I hereby grant permission to the Graduate Division of the University of California, San Francisco to release copies of my thesis, dissertation, or manuscript to the Campus Library to provide access and preservation, in whole or in part, in perpetuity.

Author Signature

3/07/2011

Date